THE EFFECT OF GLIA ON THE FORMATION OF RECURRING MOTIFS IN DISSOCIATED CORTICAL CULTURES

KWEK MENG TEE

MASTER OF ENGINEERING AND SCIENCE

LEE KONG CHIAN FACULTY OF ENGINEERING AND SCIENCE
UNIVERSITI TUNKU ABDUL RAHMAN
OCTOBER 2018

THE EFFECT OF GLIA ON THE FORMATION OF REUCRRING MOTIFS IN DISSOCIATED CORTICAL CULTURES

By

KWEK MENG TEE

A dissertation submitted to the
Department of Mechatronic and Biomedical Engineering,
Lee Kong Chian Faculty of Engineering and Science,
Universiti Tunku Abdul Rahman,
in partial fulfillment of the requirements for the degree of
Master of Engineering and Science
October 2018

ABSTRACT

THE EFFECT OF GLIA ON THE FORMATION OF RECURRING MOTIFS IN DISSOCIATED CORTICAL CULTURES

Kwek Meng Tee

Repeating patterns of neuronal activity, a potential substrate of information and memory, have been observed in various cortical structures. Whether the genesis of these recurring spatiotemporal activity patterns – or also known as 'motifs' – are the sole realm of neurons or are they also affected by glial cells in the networks remained an open question. To study the potential effect of glia in motif formation, the bursting activity in three types of cultures – high-glial culture (HGC), low-glial culture (LGC), and glia-free culture (GFC) was examined. Bursts were clustered into different groups based on their spatiotemporal structures during the initiation phase, using an algorithm that has been shown to be effective in tracking recurring patterns *in vitro*. The analysis revealed motifs of bursts with distinct spatiotemporal activity patterns in all types of cultures at both young and mature stages, but with different propensity and precision of conservation. Meanwhile, the spatiotemporal structure of bursts and network synchrony were also affected by the presence of glia and its density in the cultures. These findings demonstrate the relevance and significance of glia in modulating the spatiotemporal activity patterns of neuronal networks.

ACKNOWLEGEMENTS

Throughout my postgraduate life, I have received many helps from different people. Without them, my research would not be possible to complete.

First, I would like to express my appreciation to my supervisor, Dr Mok Siew Ying. She has been guiding, motivating, and helping me during all time of my study, including at this later stage of my thesis writing. I could not have imagined having a better mentor for my Master. Besides, I would also like to thank my co-supervisor, Prof. Dato' Ir. Dr. Goh Sing Yau for his valuable advice and support. It is because of his generosity that I am able to attend the overseas conference. A special thanks to my second co-supervisor, Professor Lim Yang Mooi for her inputs to my project, as well as her kindness in providing me a good workplace to conduct my experiments.

I am grateful to the laboratory staffs, Mr. Kho Soon Hang, Ms. Heng Sze Lu, and Ms. Grace for their patience and guidance in operating some of the equipment in the laboratory. Besides, I would like to thank Dr Wong Voon Hee for his advice in statistical analysis.

I am also thankful to my fellow friends at UTAR, Lee Jia Ji, Soh Ying Wei, Catherine Goh, and Donica, for their help and friendship. Last but not least, a huge thank you goes to my family for their endless support and faith in me throughout my postgraduate life. Without them, I can hardly complete my master study.

APPROVAL SHEET

This dissertation entitled "**THE EFFECT OF GLIA ON THE FORMATION OF RECURRING MOTIFS IN DISSOCIATED CORTICAL CULTURES"** was prepared by KWEK MENG TEE and submitted as partial fulfillment of the requirements for the degree of Master of Engineering and Science at Universiti Tunku Abdul Rahman.

Approved by:

_____

(Dr. Mok Siew Ying) Date:……..
Supervisor
Department of Mechatronic and Biomedical Engineering
Lee Kong Chian Faculty of Engineering and Science
Universiti Tunku Abdul Rahman

_____

(Prof. Dato' Ir. Dr. Goh Sing Yau) Date:……..
Co-supervisor
Department of Mechanical and Material Engineering
Lee Kong Chian Faculty of Engineering and Science
Universiti Tunku Abdul Rahman

_____

(Prof. Dr. Lim Yang Mooi) Date:……
Co-supervisor
Department of Pre-clinical Sciences
Faculty of Medicine and Health Sciences
Universiti Tunku Abdul Rahman

LEE KONG CHIAN FACULTY OF ENGINEERING AND SCIENCE

UNIVERSITI TUNKU ABDUL RAHMAN

Date: _____

SUBMISSION OF DISSERTATION

It is hereby certified that **KWEK MENG TEE** (ID No: **15UEM07429**) has completed this dissertation "**THE EFFECT OF GLIA ON THE FORMATION OF RECURRING MOTIFS IN DISSOCIATED CORTICAL CULTURES**" under the supervision of **Dr. MOK SIEW YING** (Supervisor) from the Department of Mechatronics and Biomedical Engineering, Lee Kong Chian Faculty of Engineering and Science, **Prof. Dato' Ir. Dr. GOH SING YAU** (Co-Supervisor) from the Department of Mechanical and Material Engineering, Lee Kong Chian Faculty of Engineering and Science and **Prof. Dr. Lim Yang Mooi** (Co-supervisor) from the Department of Pre-clinical Sciences, Faculty of Medicine and Health Sciences.

I understand that University will upload softcopy of my dissertation in pdf format into UTAR Institutional Repository, which may be made accessible to UTAR community and public.

Yours truly,

_____
(KWEK MENG TEE)

DECLARATION

I hereby declare that the dissertation is based on my original work except for quotations and citations which have been duly acknowledged. I also declare that it has not been previously or concurrently submitted for any other degree at UTAR or other institutions.

Name _____

Date _____

TABLE OF CONTENTS

LIST OF TABLE

LIST OF FIGURES

LIST OF ABBREVATIONS

Ara-C	cytosine arabinoside
Anti-GFAP	anti-glial fibrillary acidic protein
Anti-MAP2	anti-microtubule associated protein 2
ASDR	array-wide spike detection rate
CO_2	carbon dioxide
DAPI	4',6-diamidino-2-phenylindole
ddH_2O	double-distilled water
DIV	days *in vitro*
E18	embryonic day 18
ISI	inter-spike-interval
MEAs	multi-electrode arrays
GFC	glia-free culture
LDHGC	low density high glial culture
HGC	high glial culture
LDLGC	low density low glial culture
LGC	low glial culture
PBS	phosphate buffered saline
PEI	poly-ethylene-imine

CHAPTER 1

INTRODUCTION

One of the major goals in neuroscience is to understand information processing and storage in the brain. These complex brain functions have been explored using different approaches, ranging from studies of smaller brains in insects (Delcomyn, 1976; Fujita et al., 2013) to functional imaging using human models (Knutson et al., 2000; Zotev et al., 2014), all of which have yielded a great deal of fascinating information. A big drawback with these approaches, however, is that they are less amenable to observation and manipulation. In the current work, the capability of cell type manipulation in simpler *in vitro* networks was harnessed to gain greater insight into the role of glia in regulating the dynamics of spatiotemporal neuronal activity – including the recurring sequences of action potentials – a potential substrate of memory, information coding and retrieval, in the nervous system.

Recurring spatiotemporal neural activities, or also known as motifs, have a long history of inquiry *in vivo* (Lee and Wilson, 2002; Villette et al., 2015) and in brain slices (Ikegaya et al., 2004; Matsumoto et al., 2013). Recent studies reported that they also exist in self-assembled networks that are lacking of intrinsic architecture of the brain circuitry. Besides present in the spontaneous activity of the dissociated networks (Segev et al., 2004; Sun et al., 2010; Schroeter et al., 2015), motifs of different spatiotemporal structures can also be induced using pharmacological agents (Baruchi and Ben-Jacob, 2007),

giving rise to a potential avenue for studying the repeating neural patterns *in vitro*. Up till now many different studies (Rolston et al., 2007; Raichman and Ben-Jacob, 2008; Yada et al., 2016) have been performed to unravel the underlying mechanisms of these recurring motifs, but the focus has been mainly on the neurons, as well as the networks that they formed. The role of glia, on the other hand, has been largely dismissed.

Glia are the non-neuronal cells that make up about half the total volume of the nervous system. Because they are not electrically excitable, they were traditionally thought to provide primarily structural and metabolic support for neurons. Emerging evidence in the recent decades, however, demonstrated that glia are endowed with powerful mechanisms which enable them to participate in various signaling and regulation processes in the nervous system (Perea and Araque, 2010; Newman, 2015). Importantly, malfunctions of glia and impaired neuron-glia interactions have also been implicated to underlie various pathological diseases (Phatnani and Maniatis, 2015; Kaminsky et al., 2016). Nonetheless, the effect of glia on the regulation of the spatiotemporal activity dynamics is not well-characterized.

The present study aims to investigate how the spatiotemporal neural activity dynamics, particularly the recurring spatiotemporal motifs, are affected by glia. To allow for direct comparison on the effect of glia on neuronal activity, three types of cultures – high glial culture (HGC), low glial culture (LGC), and glia-free culture (GFC) were grown. These cultures were grown on multi-electrode arrays (MEAs) to enable long-term recording of

electrical activity from multiple sites of the networks. Analysis was performed to identify the propensity of the emergence of motifs in the spontaneous bursts, as well as their precision of conservation in the earlier (11-21 DIV) and later stages of network development (25-32 DIV). Besides, the effects of glia on the spatiotemporal structures of bursts and synchrony throughout network development were also examined.

CHAPTER 2

LITERAUTRE REVIEW

This chapter provides a description of the current electrophysiological techniques, and a brief review of the suggested mechanisms of motif formation, the motif detection techniques, and the proposed roles of glial cells in neuronal networks.

2.1 Dissociated Neuronal Cultures on MEAs

Dissociated neuronal culture represents a simplified biological model of the brain and had been utilized in many neurobiological studies over the past decades (Kamioka et al., 1996; Pasquale et al., 2008; Ju et al., 2015). It is well noted that although these cultures do not possess the 3-dimensional architecture of the intact brain, the connectivity between neurons is not random. Instead, the neurons can self-organize to form a small-world network (Rolston et al., 2007; Sun et al., 2010; Mok et al., 2012). At the same time, they also retain electrical, morphological and pharmacological properties of neuronal networks *in vivo* (Dichter, 1978; Jimbo and Robinson, 2000; Wagenaar, et al., 2005; Sibarov et al., 2016). Several techniques are available for measuring the electrophysiological activity of these cultured networks, among those include patch clamp, calcium imaging, and MEAs — each of which presents as a powerful technique for assessing neuronal activity.

The patch clamp offers the advantage for measuring single-cell activity including subthreshold events that are undetectable using the extracellular recording technique (Lampl et al., 1999). However, this technique fails to provide information about the spatiotemporal dynamics of neuronal networks as there is a limited number of cells that can be patched at the same time (Reppel et al., 2004). Also, this technique is limited to short-term studies as neurons are invariably damaged through the intimate contact with the micropipette (Wagenaar et al., 2006).

Studying population dynamics with single cell resolution is the major strength of the calcium imaging technique (Russell, 2011). This technique enables measurements of calcium dynamics of cells including those that do not fire action potentials but are electrophysiologically active, such as glia (Hirase et al., 2004; Russell, 2011). Nonetheless, this method provides only indirect observation of neuronal spikes with limited time resolution, as the induced calcium transients generally respond at an order of magnitude slower than the neuronal activity (Badura et al., 2014; Lock et al., 2016). Besides, the extraction of action potential from calcium signals was highly dependent on the image quality (Grienberger and Konnerth, 2012).

The MEA is designed for measurement of the extracellular activity of neurons. As opposed to patch clamp, this technique enables recordings from large ensembles of neurons from the networks. Importantly, neurons are not destructed during recording due to the non-invasive nature of the technique, which allows the researchers to keep track of the neuronal activity over a long

time scale (Wagenaar et al., 2006; Sun et al., 2010; Bikbaev et al., 2015). The key disadvantage of this technique, however, is its inability to resolve signals at the cellular level (Rey et al., 2015). This technique is therefore suitable only for studies of population dynamics that are based upon multi-unit data instead of single-unit activities.

2.2 Spontaneous Bursts and the Emergence of Recurring Motifs

Spontaneous bursts were observed both *in vivo* (Luczak et al., 2007; Grienberger et al., 2014) and *in vitro* (Latham et al., 2000; Bikbaev et al., 2015), suggesting their functional role in neuronal networks. It is also believed that neurons transfer information in the form of spontaneous bursts to enhance the reliability of communication between themselves (Izhikevich et al., 2003).

Although a vast variety of burst structures and patterns was observed throughout the culture development, several studies have showed that the spatiotemporal structures of spontaneous bursts were significantly repeatable (Lee and Wilson, 2002; Segev et al., 2004; Madhavan et al., 2005; Luczak et al., 2007; Rolston et al., 2007; Schroeter et al., 2015). Such repeating patterns of neuronal activity, or 'motifs' were robust that they remained for hours and were believed to serve as information substrate or memory templates in neuronal networks (Madhavan et al., 2007; Villette et al., 2015).

Until now, several hypotheses have been proposed to account for the emergence of these recurring motifs, including intrinsic mechanisms of

neuronal circuits (Ikegaya et al., 2004), networks with different spatial morphologies (Raichman and Ben-Jacob, 2008), spontaneous emergence in self-organizing networks (Rolston et al., 2007; Sun et al., 2010), and sequential activation of neuronal sub-population (Yada et al., 2016). On the other hand, there were also studies which reported that these activity patterns could be altered by electrical stimulation (Madhavan et al., 2007; Pasquale et al., 2017), and can even be imprinted into cultures using chemical stimuli targeting at specific groups of neurons (Baruchi and Ben-Jacob, 2007), suggesting that the dynamical flow of neuronal information in the networks can be modified by external inputs.

While the above studies have provided much useful insights towards understanding of the mechanisms that may lead to the emergence of recurring motifs, the focus has been mainly on neurons and the networks that they formed. Given that there is increasing evidence which showed that glia played an important role in modulating network activity (Pfrieger and Barres, 1997; Boehler et al., 2007; Feldt et al., 2010; Huang et al., 2015; Chever et al., 2016), it is tantalizing to ask whether these non-neuronal cells also affect the spontaneous generation of recurring motifs in the networks.

2.3 Methods for Identification of Recurring Motifs

Various techniques have been developed and used for identifying the repeating motifs from the spontaneous network activity. A brief description of these techniques is presented here.

2.3.1 Spike Rate Characteristics

Madhavan et al. (2005) identified repeating motifs based on the firing intensity of neurons in the bursting activities. The number of spikes that occur on each electrode within a burst was computed, and bursts with similar firing rate on individual electrodes were clustered together. Despite of its ease of implementation (Yamashita, 2005; Oyelade et al., 2010), the information about temporal delay between neurons is lacking. This method is therefore less ideal as the timing of neuronal firing is thought to encode information more effectively compared to spike rate (Mokeichev et al., 2007; Srivastava et al., 2017).

2.3.2 Correlation between Spike Trains

Segev et al. (2004) and Yada et al. (2016) measured the similarity between constituent bursts based on the average correlations between their neuronal spike trains. Bursts with high similarity in the patterns of interneuron spatial correlations were clustered together and identified as a motif. Compared to the previous approach, this method demonstrates better resolution as temporal delay between neuronal spike trains was taken into consideration. However, the resultant correlations were strongly dependent on burst intensity and duration.

2.3.3 Template Matching Algorithm

Template-matching algorithm has been shown to be effective in identifying recurring neural patterns both *in vivo* (Nádasdy et al., 1999) and *in vitro* (Rolston et al., 2007; Sun et al., 2010). The algorithm first searched for repeating spike sequences within a specific time window and marked them as reference templates. These templates were then shifted throughout the recorded data and their recurrences were determined. This method provides a robust measure of the recurrence of spike sequences on the timescale of milliseconds to seconds. A major drawback of this method, however, is that it is time-consuming, as one minute of multielectrode data would need about thirty minutes to analyze on a standard desktop computer (Rolston et al., 2007).

2.3.4 Activation Patterns

In contrast to the previous methods which take into account the activity of the entire spike trains, Raichman and Ben-Jacob (2008) identified recurring motifs based solely on the first spike of neurons participating in the bursts. The latency between neurons during burst initiation was computed and used as the measure of comparison with other bursts. This idea of including only the neuronal activation pattern in the motif analysis has effectively reduced the spatio-temporal structure of the bursts, eliminating the bias given rise by the firing intensity of neurons and burst duration. Importantly, timings of the spikes has also been shown to be more precise in the starting point of the spike

trains, in both spontaneous (Luczak et al., 2007) and evoked bursts (Jimbo and Robinson, 2000).

2.4 The Role of Glial Cells in Neuronal Networks

Traditionally, glial cells were believed to play solely supporting roles in neuronal networks, such as guiding neurons to targeted areas (Powell and Geller, 1999), maintaining ionic balance (Schwartzkroin et al., 1998), and supporting energy metabolism homeostasis (Tsacopoulos and Magistretti, 1996). There is increasing evidence in the recent years, however, which shows that glial cells, particularly astrocytes, play an active role in the modulation of neural activity. Although being unable to generate action potentials, glia affect the development of neurons by enhancing their synaptic efficacy (Pfrieger and Barres, 1997). They also exhibit calcium transients which can directly modulate the intracellular calcium dynamics in neurons (Newman and Zahs, 1998; Takayama et al., 2009; Sasaki et al., 2014). Additionally, glial cells release gliotransmitters in response to neural activity, which allow them to involve in the integrative processes within neural networks (Anderson and Swanson, 2000; Yang et al., 2003; Zhang et al., 2003; Newman, 2015). More recently, they have also been implicated to participate in the modulation of synaptic plasticity (Eroglu and Barres, 2010; Stogsdill and Eroglu, 2017); an ability that was long thought to be possessed solely by neurons.

Although the functional role of glia has now been recognized, their contribution to the spatiotemporal activity dynamics of networks is unclear.

By carefully manipulating the cell type in hippocampal cultures growing on MEAs, Boehler et al. (2007) showed that added astroglia altered the spike rates and characteristics of the network bursts. In a separate work, Feldt et al. (2010) analyzed the differences in the spatiotemporal dynamics of neurons grown with both high and low densities of glial cells and detected more consistent functional structures and higher synchronization in the activity of cultures with higher glial density. Similarly, Huang et al. (2015) reported more synchronized burst activity in neuron-glia mixed cultures compared to glia-free cultures.

CHAPTER 3

METHODOLOGY

3.1 Cell Culture

Dissociated cortical cultures were prepared from cortical hemisphere of E18 embryonic rats (BrainBits^{TM}). First, cortical tissues were dissociated using 0.25% trypsin at 37°C for 15 minutes and triturated using Hank's balanced salt solution with 10% Equine serum. The dissociated cells were then centrifuged onto bovine serum albumin (1% in 1X PBS) at 150 x g for 6 minutes and the resulting pellet was resuspended in Neurobasal medium supplemented with 2% B27, 5% Equine serum, and 1 mM Glutamax. Cells were diluted to achieve a final concentration of 4000 cells/µL and seeded in a 50 µL drop on central area of MEAs precoated with poly-ethylene-imine (PEI). All MEAs were covered with Teflon membrane to prevent microbial infection and to minimize medium loss via evaporation (Potter, 2001).

Following plating, the cultures were divided into three groups and maintained under different conditions: the first group continued to grow in serum-supplemented medium to promote the proliferation of glia (high glial culture; HGC), the second group treated with the mitotic inhibitor, 1 µM Ara-C on 8 DIV and grown in serum-supplemented medium to maintain a minimal number of glia (low glial culture; LGC), and the third group treated with 1 µM Ara-C 24 hours after seeding to restrict the glial growth and thereafter

maintained in glia-conditioned medium (glia-free culture; GFC). Glia-conditioned medium was prepared by incubating serum-free medium with a confluent layer of glial cells (See Appendix A for details). In all cases, half of the medium was replaced every 4 to 7 days, depending on the changes in the color of the medium.

3.2 Immunostaining

To verify whether the treatment of Ara-C was successful in suppressing the growth of glia, immunostaining was performed. Cultures used for immunostaining were prepared on glass bottom dishes using the same protocol described in Section 3.1. On the days of experiment, the cultures were fixed with 4% paraformaldehyde for 10 minutes, followed by permeabilization with 0.03% Triton X-100 for 5 minutes. They were then treated with 5% bovine serum albumin for 30 minutes to reduce the background. Subsequently, the cultures were incubated with the primary antibodies anti-MAP2 (chicken, 1:1000) and anti-GFAP (mouse, 1:1000) at room temperature for 1 hour, followed by secondary antibodies Alexa Fluor 488 goat-anti-chicken (1:200) and Alexa Fluor 546 goat-anti-mouse (1:200) for 45 minutes. Lastly, they were counterstained with 1 μg/mL DAPI and mounted with Fluoromount. In between each step, the cultures were rinsed with 1X PBS for at least 3 times. Images were captured using a Nikon fluorescence microscope.

3.3 Data Acquisition

Extracellular signals were recorded using MEAs which contain 60 titanium nitride electrodes arranged in 8 X 8 square grids (MultiChannel Systems (MCS); Figure 3.1). The diameters of electrodes were 30 μm with inter-electrode spacing of 200 μm. Signals were amplified at 1100X and digitized at 25 kHz using the MCS hardware. The data were stored for offline processing using custom tools developed in Matlab.

Recordings were performed starting from the end of second week *in vitro*, when cultures constantly exhibiting spontaneous bursts. Each recording session lasted 30 minutes to 2.5 hours.

3.4 Spike Detection

To extract spikes or (multi-unit) action potentials, raw data traces were first high-pass filtered at 200 Hz. The threshold for spike detection was set at five times standard deviation of background noise on individual electrode. To accommodate for the drift in the noise level, the voltage thresholds of the electrodes were updated continuously (at every 3 minutes).

Since extracellular neuronal waveforms are often multiphasic, putative spikes recorded in close succession need to be eliminated to prevent double detection of a single event. Therefore, only the highest peak within a ±1 ms time window was accepted as a spike.

(A)

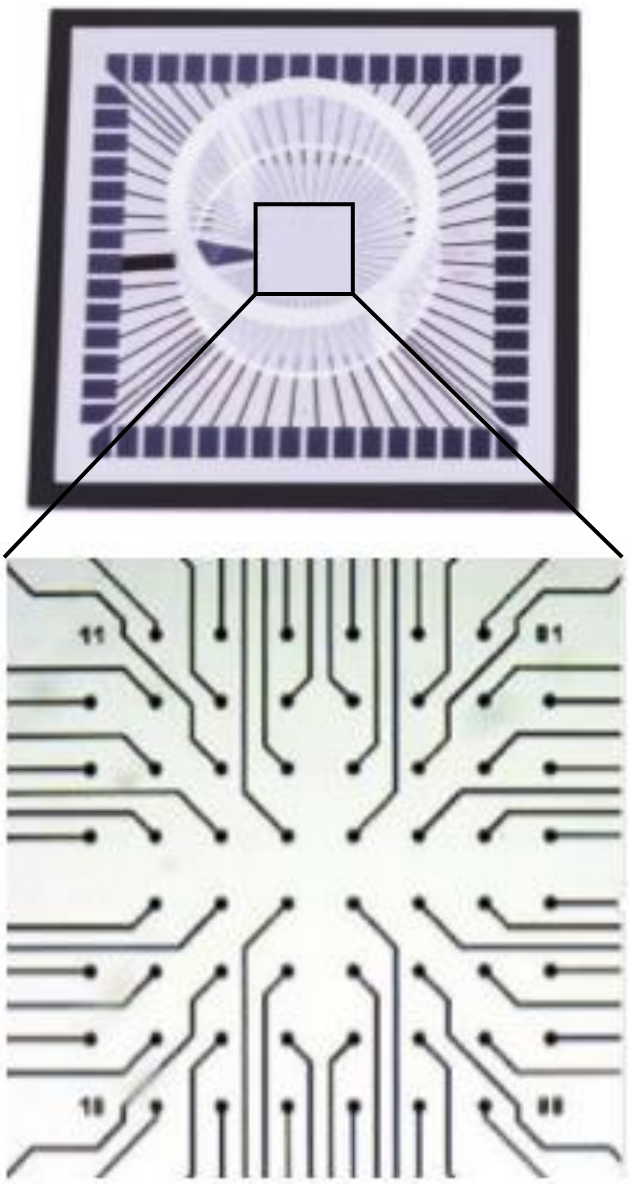

Figure 3.1: Extracellular recording using MEA. (A) MEA and the microscopic view of its central electrode area. (B) Micrograph of a dissociated neuronal culture growing on a MEA. Scale: 200 µm between electrodes. (C) Example of a typical network burst. Each box represents an electrode in the MEA.

(B)

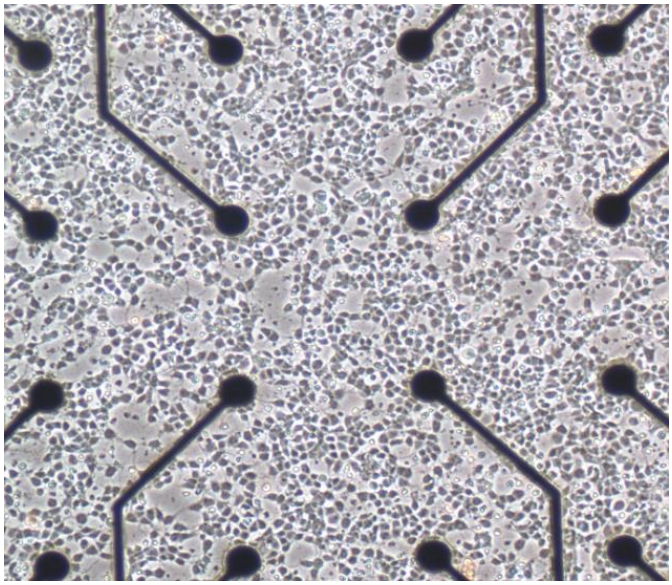

(C)

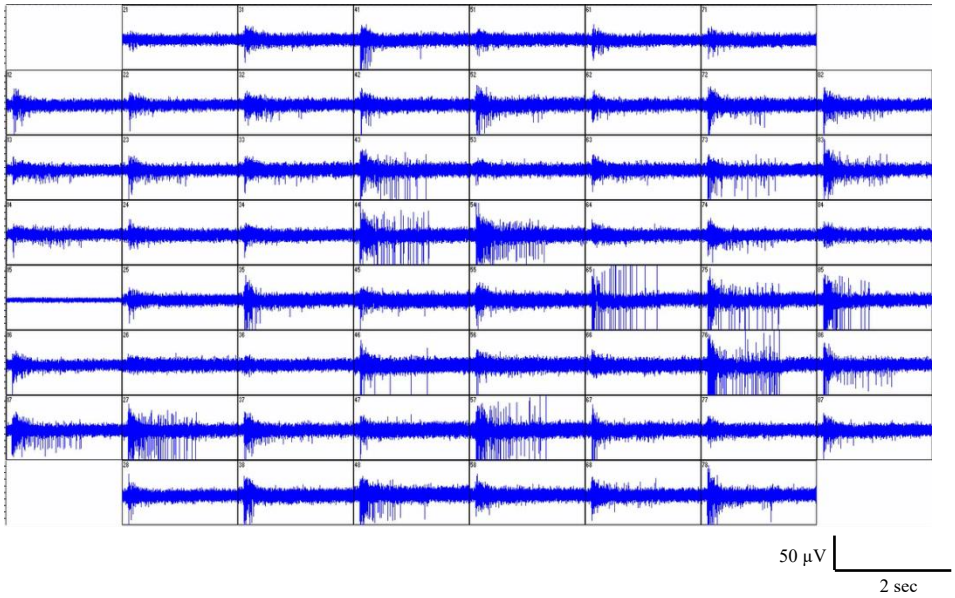

(Figure 3.1, continued)

3.5 Burst Detection

Spontaneous bursts were detected using an algorithm described by Wagenaar et al. (2005). Briefly, the activity of individual electrodes was screened to identify the time windows that contained at least four closely spaced spikes with a maximum inter-spike-interval (ISI) of 100 ms. After these 'cores' were identified, the algorithm continued to search for spikes with ISIs less than 200 ms on the same electrodes. The multiple individual electrode bursts that overlapped temporally constitute a network burst.

3.6 Identification of Recurring Motifs

A spatiotemporal motif is identified as a cluster of bursts (of a predefined size) that shared a similar activity propagation profile, as described by Raichman and Ben-Jacob (2008). This method is adapted in the present study as it was proven to be successful in identifying recurring spatiotemporal structures in previous works involving dissociated cultures (Mok et al., 2012; Pasquale et al., 2017).

To begin with, a similarity index was computed between all pairs of individual bursts. These similarity indices were computed based on the latencies during which electrodes started to record bursts (Figure 3.2A; see Section 3.6.1 for details). This produced a similarity matrix with bursts arranged in the time sequence (Figure 3.2B). To identify bursts with similar propagation patterns, the sequence of bursts in the matrix were rearranged

using the hierarchical dendrogram method. This algorithm grouped bursts with the least Euclidean distance together, forming a new matrix with highly similar bursts located closely in the reordered sequence (Figure 3.2C). Subsequently, all burst clusters each containing N_{clus} consecutive bursts in the reordered matrix were identified, where N_{clus} was set as the square root of the total number of bursts ($N_{clus} = \sqrt{N_{burst}}$). Each of this cluster was represented by the mean latency of its active electrode pairs across individual bursts, with the mean latency of electrode pair (i, j), t_{mean} (i,j) in each set of cluster defined as:

$$t_{mean}(i,j) = \frac{1}{N_{clus}} \sum_{k \in set} t_k(i,j)$$

The mean similarity within the set of burst cluster, S_{set}, was then evaluated by:

$$S_{set} = \frac{1}{N_{clus}} \sum_{k \in set} S_{burst}(t_k, t_{mean})$$

The burst cluster with the highest mean similarity was determined to be the first motif. To ensure that the subsequent motifs were well-defined from the previously determined motifs, all clusters that contained bursts belonging to the previously detected motif or with bursts showing higher similarity with the selected motif than the lowest similarity within the motif itself were removed. These steps were then repeated iteratively to search for additional motifs from the remaining clusters.

To avoid bias caused by variation in the N_{clus}, analyses for the motifs were based upon a fixed number of consecutive bursts ($N_{burst} = 80$) from each culture. Only bursts spanning at least 20 electrodes were included in the analysis.

(A)

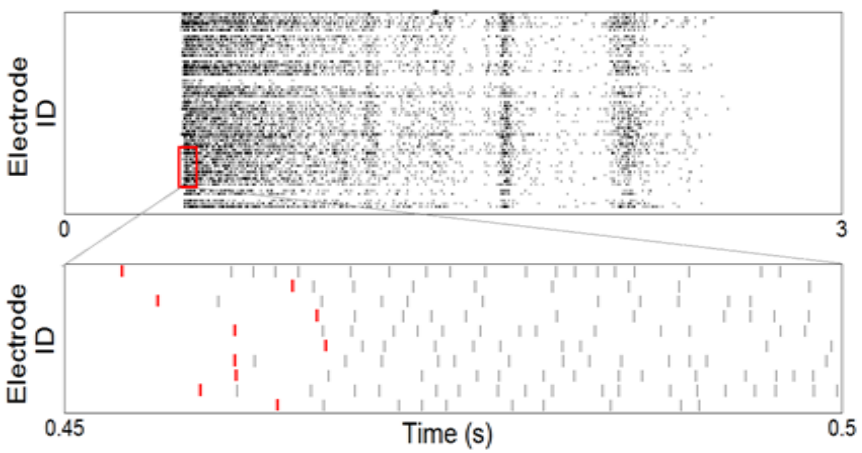

(B)

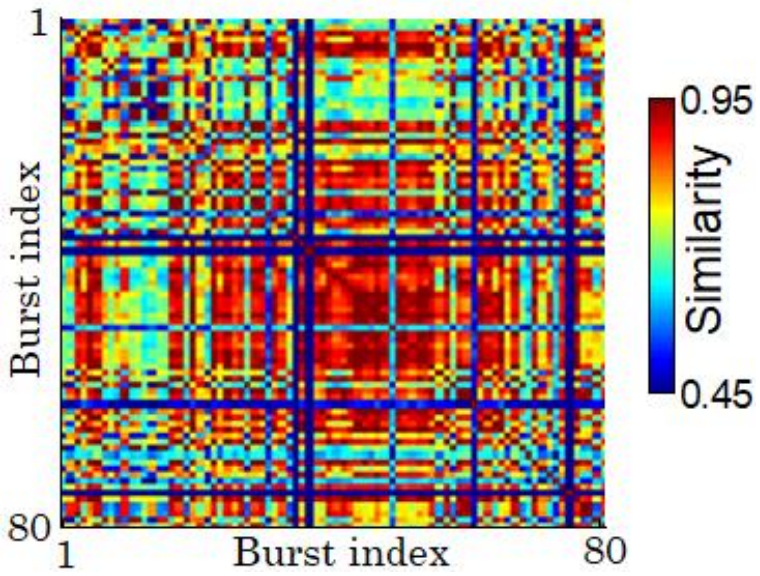

Figure 3.2: Identifying spatiotemporal motifs in the spontaneous activity. (A) Raster plot of the spiking activity for a typical network burst. The first spike from each spike train (marked in red in the inset) was extracted for estimation of the similarity index between bursts. (B) Similarity matrix of 80 consecutive bursts in one of the HGCs. (C) The same matrix shown in (B), but rearranged according to the hierarchical dendrogram method. Note clear clusters are shown along the diagonal of the matrix. '] ' denotes the identified motif. (B) and (C) are color-coded according to the bar at right. (D) The distinct spatiotemporal propagation patterns exhibited by bursts pooled from the three motifs identified in (C). Bursts from the same motifs are vertically aligned. The lines represent the propagation trajectories of the bursts through the networks, with their sequences color coded according to the bar at right. Note the high repeatability of the propagation pattern.

(C)

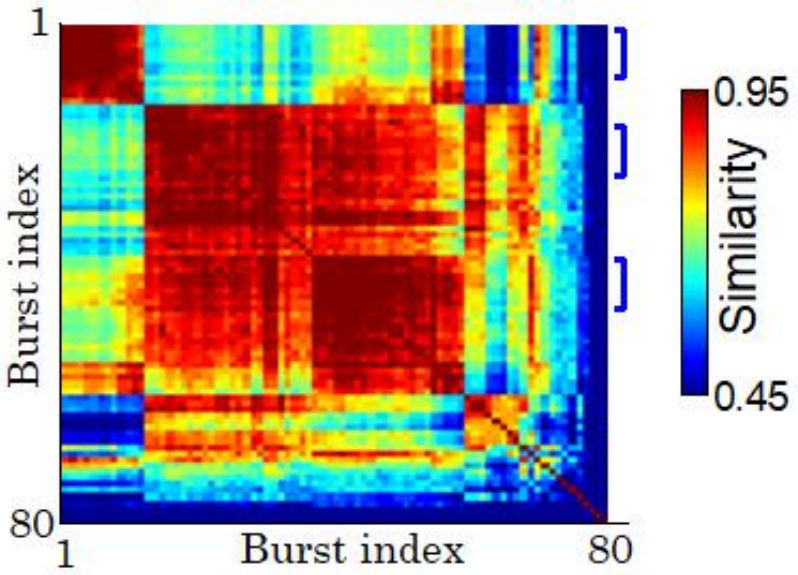

(D)

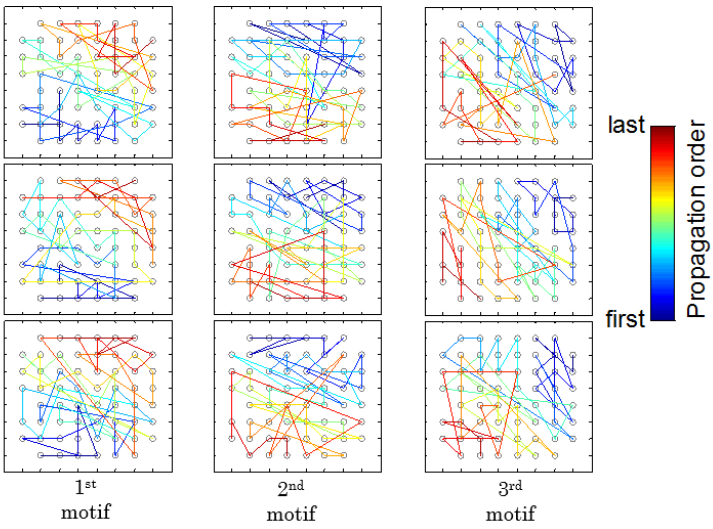

(Figure 3.2, continued)

3.6.1 Determination of Time Threshold

The similarity index between bursts *m* and *n,* $S_{burst}(m,n)$, was computed based on the relative difference in the first spikes timings on all electrode pairs (i,j):

$$S_{burst}(m,n) = \frac{1}{N_{ele}(N_{ele}-1)} \sum_{i \neq j} H(th - |t_m(i,j) - t_n(i,j)|)$$

where *H* represents the Heaviside step function; *th* represents the time threshold, and N_{ele} represents the number of electrodes that participated in both bursts.

From the above equation, it is notable that the similarity values were largely dependent on the value of *th*, the free parameter that determines the minimal accuracy in the delays between two electrodes. To identify the suitable *th*, a range of value ranging from 5 to 30 ms was tested and the changes in the similarity values were observed. As expected, the similarity between bursts increased with higher *th*, and the different activation patterns were not distinguishable with *th* greater than 10 ms (Figure 3.3). Hence, *th* was set to be 10 ms.

3.7 Network Synchrony

Network synchrony was quantified by performing cross correlation on the spike trains of all electrode pairs (Penn et al., 2016). First, all the spike trains

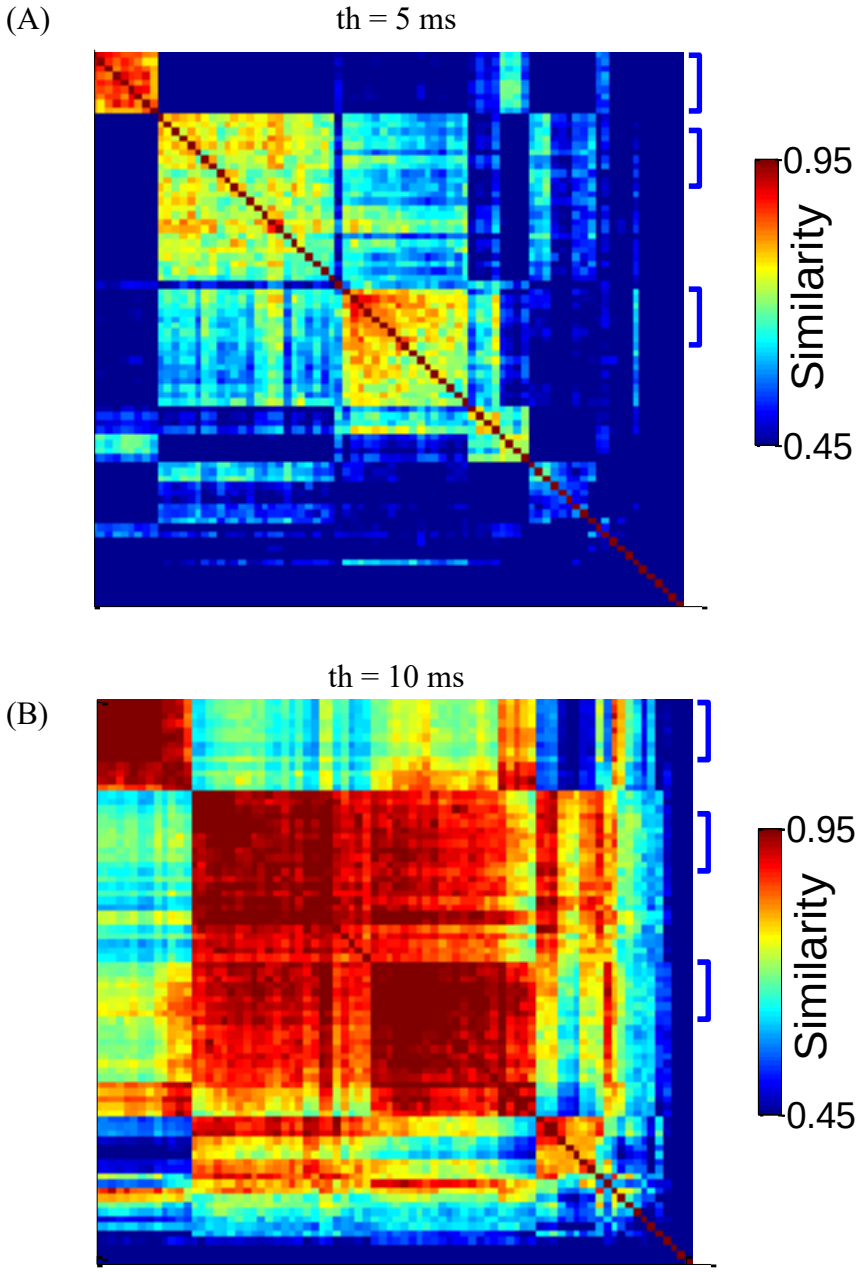

Figure 3.3: Variation in the similarity between bursts with time threshold. Images of reordered similarity matrices for the original matrix in Figure 3.2B, using four different threshold values: (A) 5, (B) 10, (C) 20 and (D) 30 ms. Each cluster marked with '] ' at the right of the matrix is identified as a motif. The matrices are colored following the bar at the right.

(C) th = 20 ms

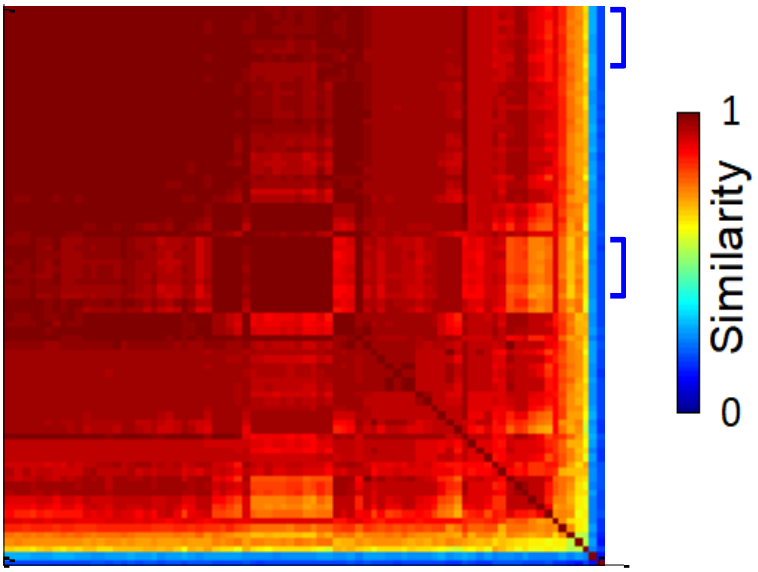

(D) th = 30 ms

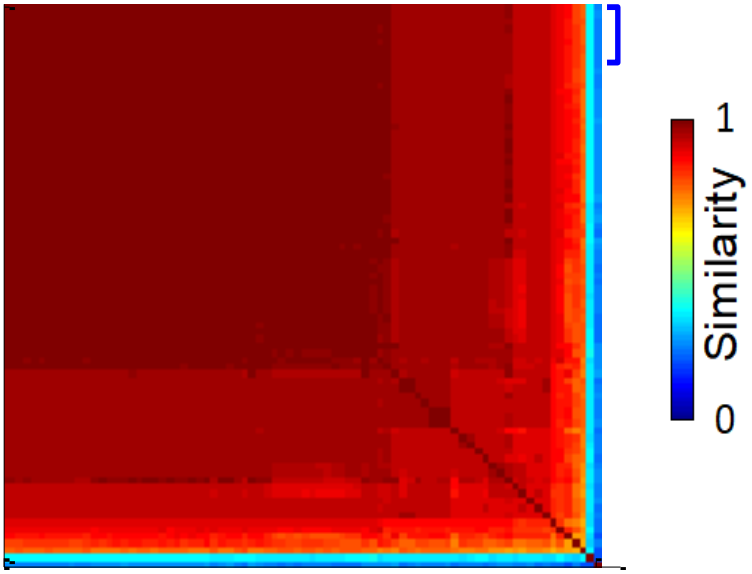

(Figure 3.3, continued)

were chopped into segments of 60 seconds. For each of the segment, correlation analysis was performed on all the electrode pairs and the peak correlation value for each pair of the electrode was extracted. The level of network synchronization was then determined by averaging across all the cross-correlation peaks.

3.8 Analysis of the Spatiotemporal Structure of Bursts

3.8.1 Burstiness Index (BI)

BI was defined as the fraction of spikes occurs in the bursts (Tropp Sneider et al., 2006), obtained by dividing the number of spikes contained in bursts by the total number of spikes. If BI is closer to 1, most of the spikes occur in the bursts and vice versa.

3.8.2 Burst Onset Phase, Burst Offset Phase, and Burst Duration

The burst onset phase (time taken for the burst to spread throughout the network), burst offset phase (time taken for the burst to be extinguished), and burst duration were computed according to Madhavan et al. (2007). Briefly, burst onset phase was the time taken for the network firing rate to increase

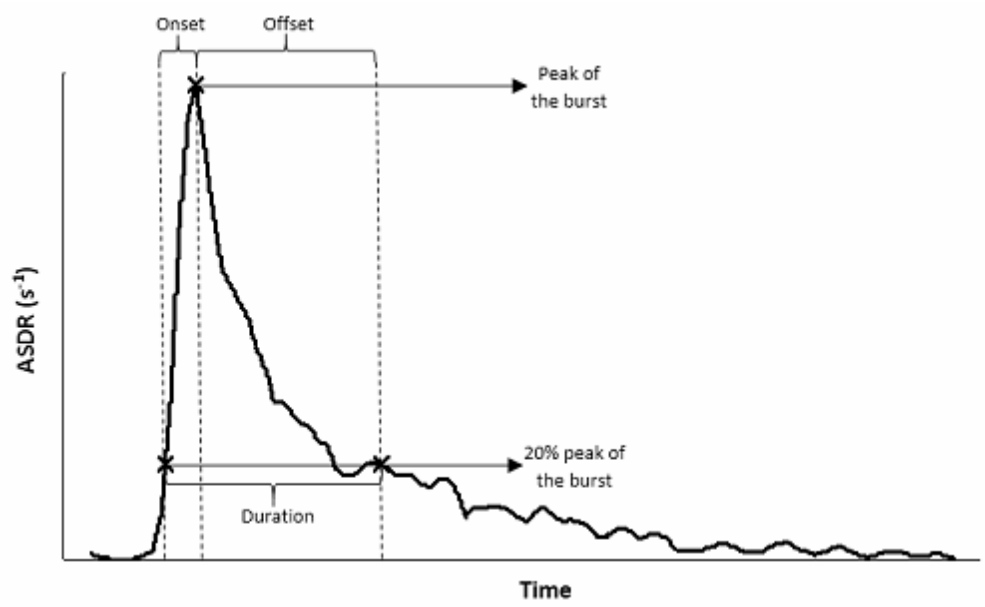

Figure 3.4: Burst onset phase, burst offset phase and burst duration of a burst in ASDR graph.

from 20% to 100% of peak ASDR, while burst offset phase was the time taken for the network firing rate to drop from 100% to 20% of peak ASDR. The burst duration was the duration between burst onset and offset phase (Figure 3.4).

3.9 Statistical Analysis

Differences in the mean burst similarity between culture groups were analyzed using the independent Student's *t*-test of the Statistical Package for the Social Sciences (SPSS) program. A significance level of 0.01 was used in this study.

CHAPTER 4

RESULTS

4.1 Regulation of Glial Density

Figure 4.1 shows the immunostaining images of cultures from the three different preparations. It is notable that the glial density was greatly reduced with the addition of Ara-C. The glial density was remarkably higher in HGC compared to LGC while there was nearly no glia observed in GFC, in both 11 and 25 DIV.

The density of neurons, on the other hand, was similar across the preparations in early days of culture but was slightly reduced in GFC towards the later stage of development, in agreement with the previous studies that glia is necessary for long-term neuronal survival (Boehler et al., 2007). Importantly, the neuronal processes appeared to be intact in all cultures, indicating that the preparations were healthy.

4.2 Effects of Glia on the Formation of Recurring Motifs

To investigate whether the spontaneous generation of recurring motifs is affected by glia in the networks, neuronal bursts from cultures of different preparations were recorded and analyzed (see Methodology). Two

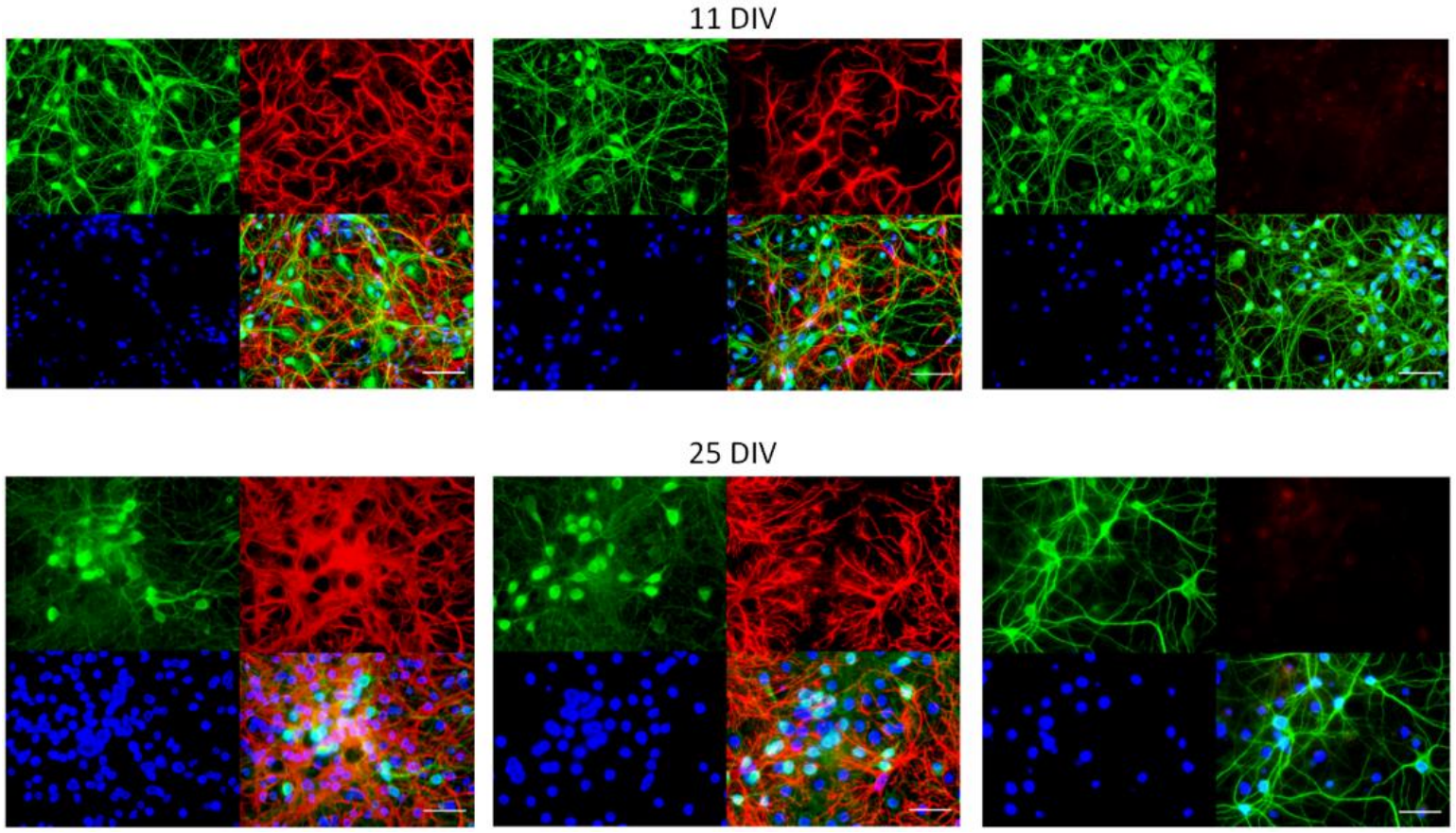

Figure 4.1: Immunostaining images of HGC (left), LGC (middle) and GFC (right) at 11 DIV (first row) and 25 DIV (second row). Neurons were labeled with anti-MAP2 (green), glial cells were labeled with anti-GFAP (red) and all were counterstained with DAPI (blue). Combined images of neurons and glia are shown in lower right of each panel. Scale bar: 50 µm.

Table 4.1: Comparison of recurring motifs in HGC, LGC, and GFC at both young and mature stages.

	Number of culture	Fraction of culture displaying motif		Number of motif	
		Young	Mature	Young	Mature
HGC	11	1.00	1.00	1-3	1-2
LGC	11	0.91	1.00	0-3	1-2
GFC	11	0.18	0.91	0-2	0-3

observations are apparent from the analysis (Table 4.1). First, distinct motifs were detected in cultures from all preparations, albeit of lower probability of occurrence in GFC. This indicates that recurring activity pattern is a general property of neuronal networks which could manifest itself in the presence or absence of glia. Second, the fraction of cultures displaying motif increased with culture age in both LGC and GFC, implying that the emergence of repeating motifs was enhanced with the maturation of neuronal networks but not glia.

While the above analysis showed that glia has no impact on motif formation, the mean burst similarity of all detected motifs from three culture groups was further computed and compared. The analysis revealed that the motifs in HGC were significantly more conserved compared to those from the other two groups at the earlier stage of development ($p<0.01$). The precision of conservation of the motifs in LGC, however, increased and became comparable to that of HGC as the cultures grew older ($p=0.32$). These results suggest that while glia was not necessary for the spontaneous generation of motifs in the networks, they were crucial for the generation of high-precision motifs (mean burst similarity > 0.7). Also, the genesis of these high-precision motifs at the earlier stage of development was highly dependent on the density

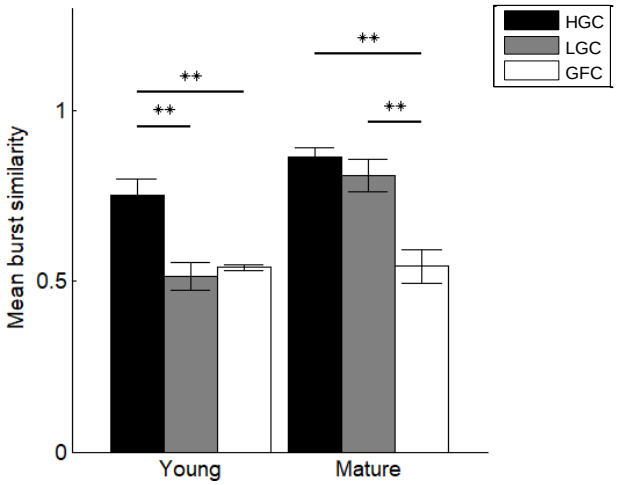

Figure 4.2: Comparison of mean burst similarity of electrode activity among HGC, LGC and GFC. Data shown are mean±SEM. ** p<0.01, independent Student's t-test.

of glia in the networks (Figure 4.2). The same was not observed at the later developmental stage, presumably because neurons played a more dominant role in regulating network activity patterns as the cultures matured.

4.3 Formation of Recurring Motifs in Cultures of Reduced Neuronal Density

The density of neurons in GFC was slightly lower compared to HGC and LGC at the later stage of development (Figure 4.1), and it is therefore unclear whether the precision of motif is also affected by neuronal density. To verify this, experiments were repeated using cultures with reduced neuronal density (half of that of the original cultures). In half of these cultures, glia were allowed to grow freely (low density high glial cultures (LDHGC); n=7) while the other half was treated with Ara-C on 8 DIV to keep a low number of glia (low density low glial cultures (LDLGC); n=6). The similar trend that was

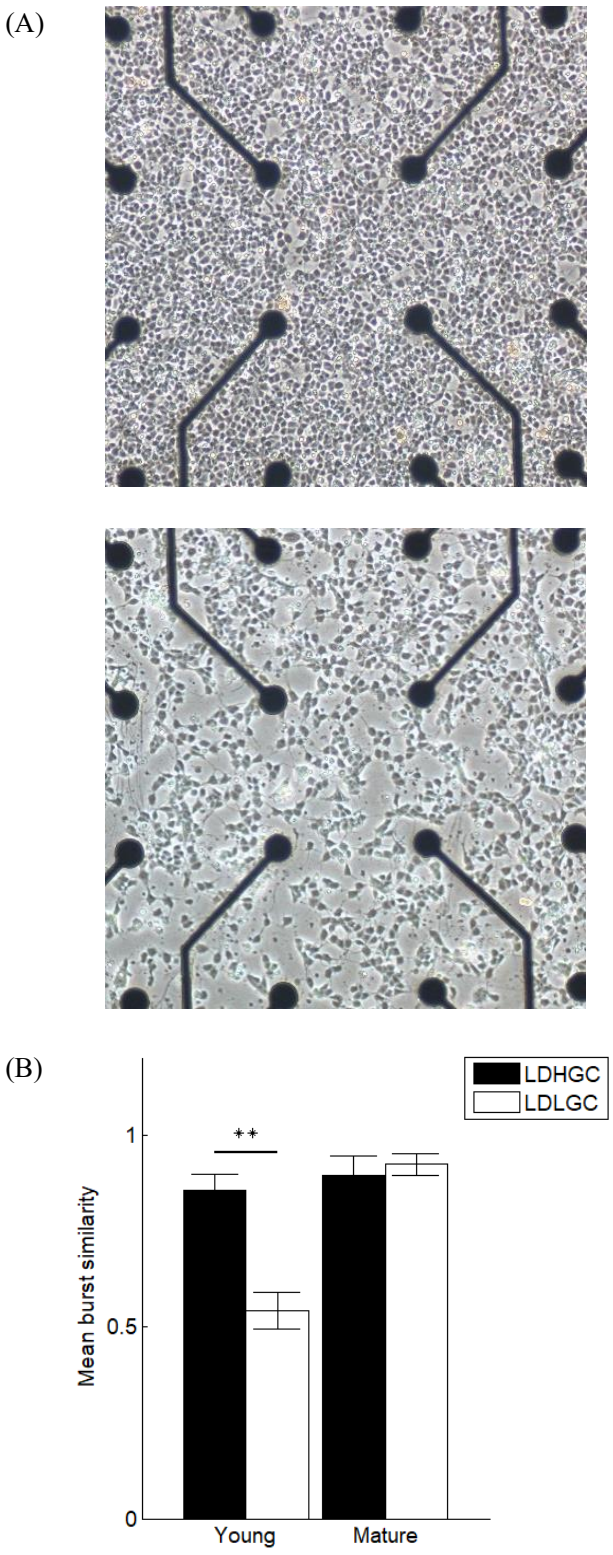

Figure 4.3: Effects of reduced neuronal density on spatiotemporal motifs. (A) Micrographs of culture with original neuronal density (top) and reduced neuronal density (bottom). (B) The mean burst similarity of the motifs developed in LDHGC and LDLGC. Data shown are mean±SEM. ** p<0.01, independent Student's t-test.

exhibited in HGC and LGC was observed (Figure 4.3B). All the networks with reduced neuronal density displayed recurring motifs, and that the mean burst similarity of LDHGC was significantly higher than LDLGC at young but not mature stages (young: $p<0.01$; mature: $p=0.65$). This confirmed that glia enhanced the spontaneous generation of recurring motifs independently from neuronal density.

4.4 Effects of Glia on the Spatiotemporal Structure of Bursts and Network Synchrony

To gain more insight into the effects of glia on the network activity, the level of network synchronization as well as the spatiotemporal structure of bursts arising from the three groups of cultures throughout network development were further compared. The effects of glia on some of these parameters have been addressed in earlier studies (Pfrieger and Barres, 1997; Feldt et al., 2010; Huang et al., 2015), but were based upon comparisons either between neuronal cultures in the presence/absence of glia or between cultures of high/ low glial density. In the following section, changes across three types of cultures were (HGC, LGC, and GFC) compared.

4.4.1 Burst Rate and Interburst Interval

All cultures were dominated by bursting activities at the second week *in vitro*, with similar increasing trend observed across the three culture groups throughout development. As shown in Figure 4.4A, the propensity of bursting

was not affected by glial cells, in agreement with Boehler et al. (2007). The duration of interburst interval steadily decreased as the cultures matured, but showing no noticeable difference among the different culture groups (Figure 4.4B).

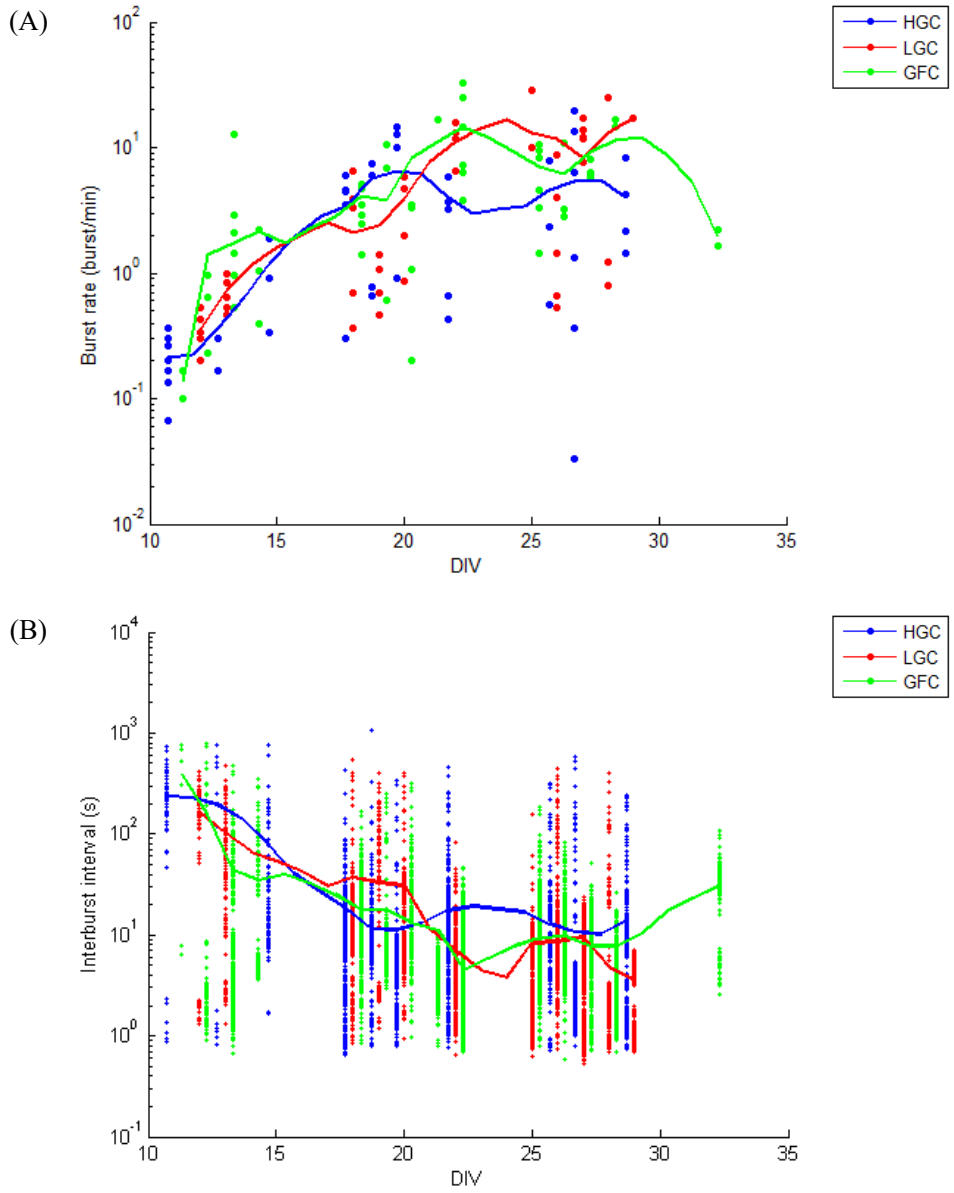

Figure 4.4: Developmental changes of (A) burst rate and (B) interburst interval in cultures. Every point from (A) denotes a value from an individual culture, and every point from (B) denotes a value from an individual burst. The lines represent the interpolated average.

4.4.2 Level of Burstiness

To examine the global behavior of the networks, including the activity outside the bursts, BI of the three culture groups was computed. The analysis showed that the level of burstiness fluctuated somewhat throughout development, but was in general higher in HGC and LGC (Figure 4.5), in agreement with Huang et al. (2015).

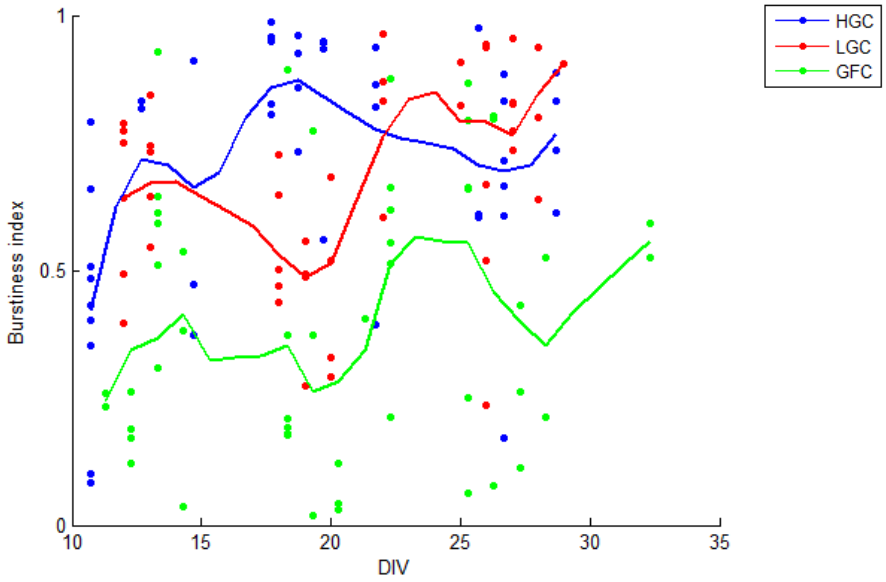

Figure 4.5: Development of burstiness index in cultures. Every point denotes a value from an individual culture and the lines are interpolated average.

4.4.3 Burst Size

While the burst rate was relatively similar across the three culture groups, the size of the bursts was considerably different. The formation of large-size bursts was enhanced in cultures of high glial density, as reflected by (1) number of constituent spikes contained in the bursts and (2) number of participating electrodes in the bursts (Figure 4.6).

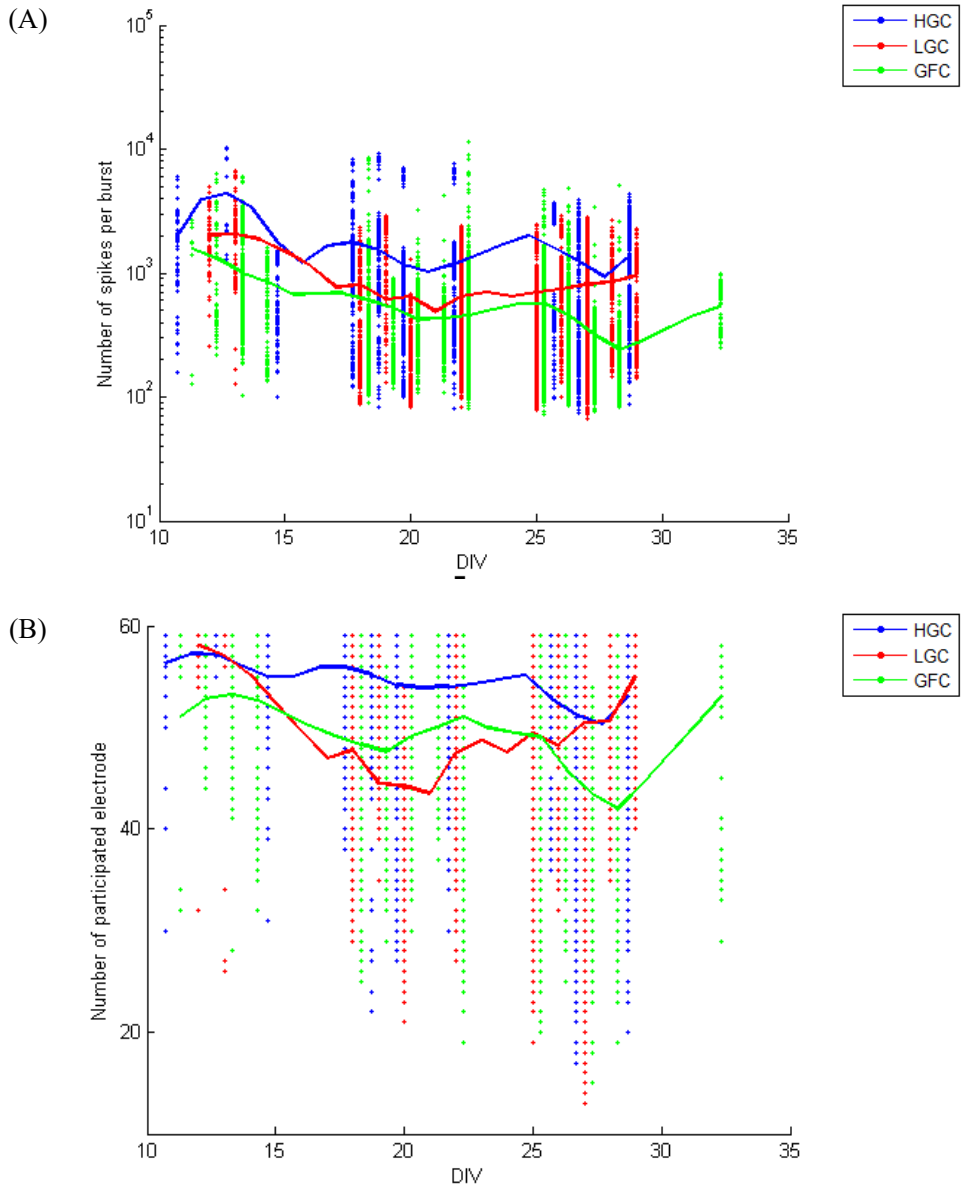

Figure 4.6: Development of burst size in cultures. (A) Number of spikes per burst. (B) Number of participated electrode in a burst. Every point denotes a value from an individual burst and the lines represent the interpolated average.

4.4.4 Burst Onset Phase, Burst Offset Phase, and Burst Duration

The burst onset and offset phases were remarkably longer in GFC compared to the other two groups of cultures throughout development (Figure 4.7), indicating that the propagation of burst activity was greatly enhanced by glial cells. Similarly, the total duration of bursts were substantially longer in GFC

(A)

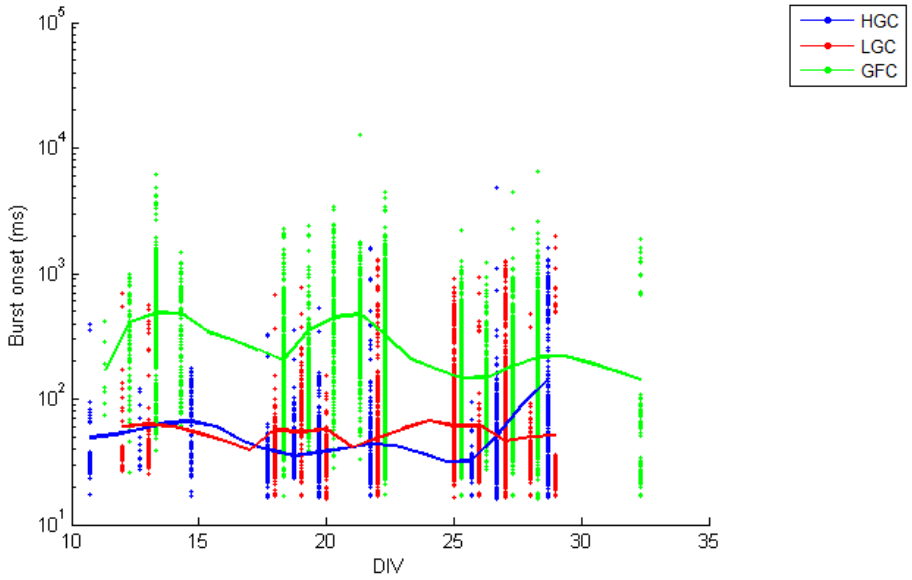

(B)

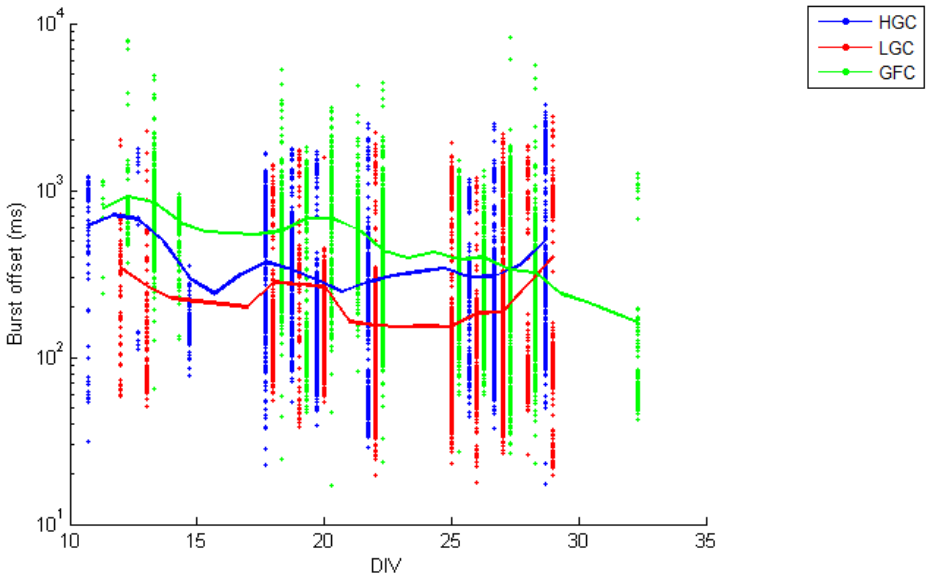

Figure 4.7: Development of burst shapes in cultures. (A) Burst onset phase. (B) Burst offset phase. (C) Burst duration. Every point denotes a value from each burst and the lines are interpolated average.

(C)

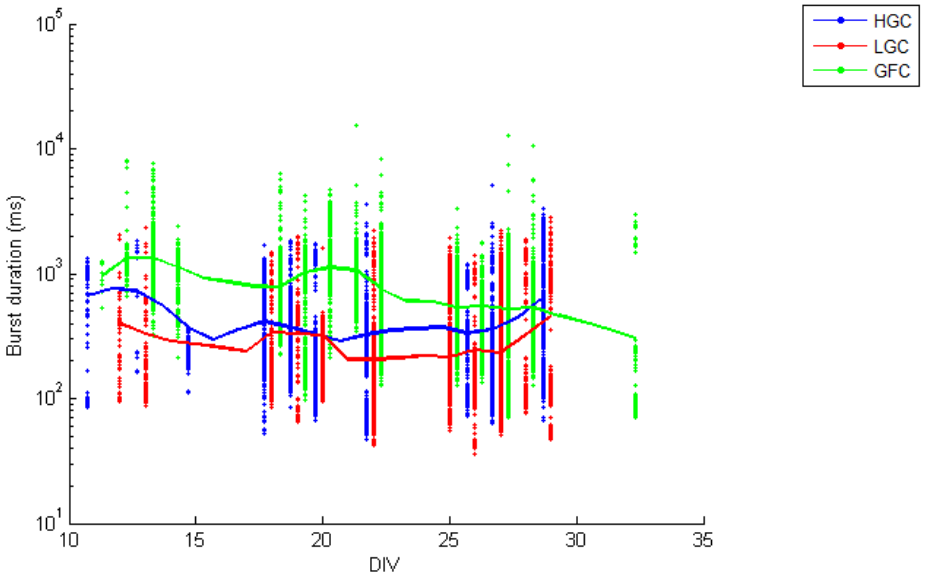

(Figure 4.7, continued)

compared to HGC and LGC (Figure 4.7C).

4.4.5 Network Synchrony

Large-scale synchronized events are the characteristic activity of dissociated cultures, but the level of synchronization of network activity varied with culture type and age (Figure 4.8). To quantify the synchronization among activities of the different electrodes, cross-correlation analysis was performed (Figure 4.9). HGC showed significantly higher degree of network synchronization compared to GFC, in agreement with previous study (Huang et al., 2015). In contrast with Feldt et al. (2010), however, no substantial difference was observed in the network synchrony between HGC and LGC.

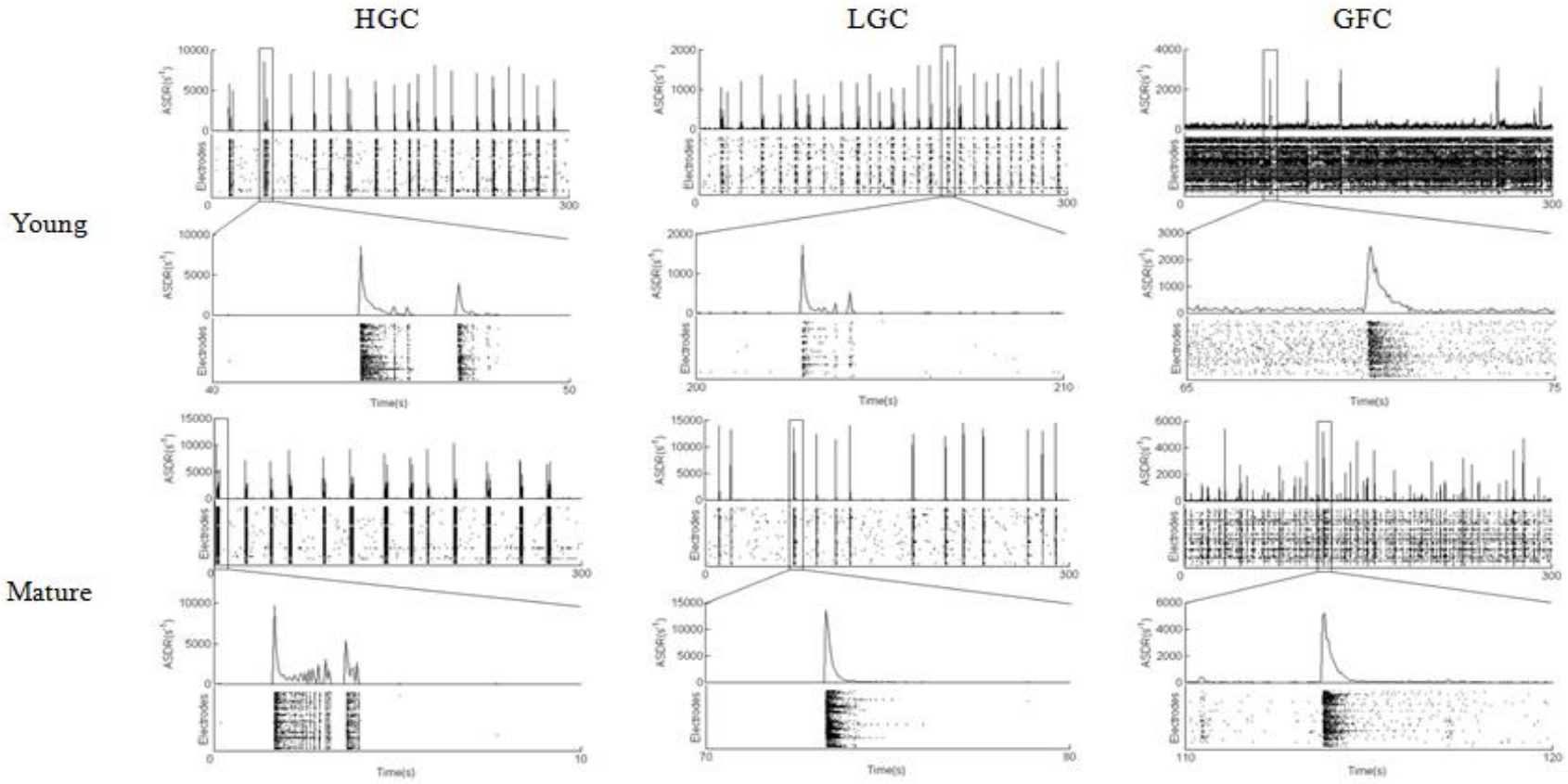

Figure 4.8: Development of spontaneous activity in HGC (left), LGC (middle) and GFC (right) at young (top) and mature stages (bottom). Each figure showed the ASDR and the simultaneous raster plot with respective culture. Insets are the magnified view of a single burst.

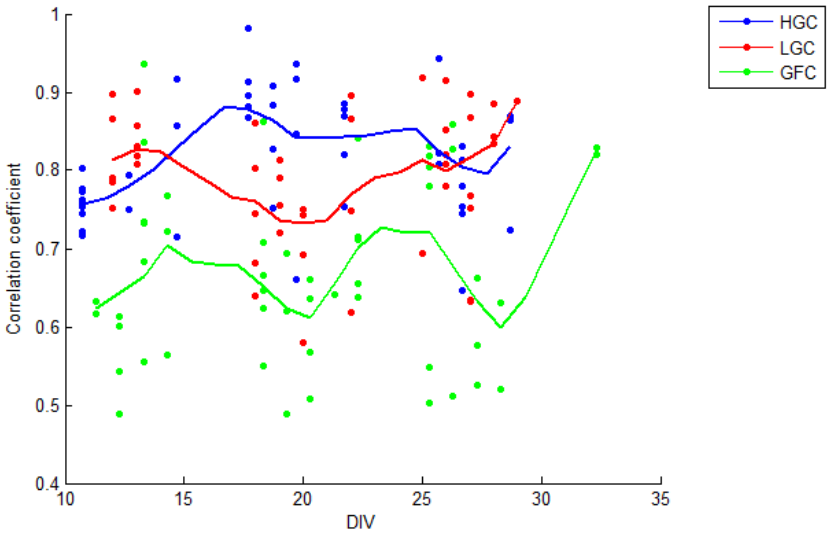

Figure 4.9: Development of neuronal synchrony in cultures. Every point denotes a value from individual culture and the lines are interpolated average.

CHAPTER 5

DISCUSSION

5.1 Discussion

The presence of precisely timed spatiotemporal patterns in the cultured networks activity has been proposed in previous works (Ikegaya et al., 2004; Rolston et al., 2007; Sun et al., 2010; Yada et al., 2016), asserting the idea that they are a general property of self-assembled networks that do not require the intrinsic brain architecture. However, all these studies were performed using cocultures of neurons and glia, and it is therefore unclear whether the genesis of these activity patterns is the sole realm of neurons, or also affected by the glial cells in the networks. In the present study, the activity dynamics of three types of cultures – HGC, LGC, and GFC were compared, in order to delineate the role of glia in the above context.

Various techniques have been developed to identify these hidden spatiotemporal structures in the networks, each based on a primary criterion. The technique adopted in the present work was based upon the latency of the first spikes on every electrode in the bursts (Raichman and Ben-Jacob, 2008), in order to prevent bias caused by the large variations in the burst size and duration (see Section 4.6). However, instead of using neuronal data as in some studies, the analysis was performed using electrode data, as multi-unit activities from biological networks were shown to be more robust and reliable (Supèr and Roelfsema, 2004; Stark et al., 2007; Mok et al., 2012).

Regardless of the presence/absence of glia and their density, most of the cultures that were examined showed the presence of motif(s), but with different propensity and precision of conservation. Since the current measure tracked motifs of similar initiation patterns and transmission of spike activity is mediated by network connectivity, the results suggest that glia may have modulated the formation of spatiotemporal motifs through regulation of the anatomical and functional connectivity of the networks. The increased variance in the initiation patterns of GFC compared to the other two groups also suggest that neuron-glia interactions play a critical role in modulating network activity, although many of the effects were also attributed to the soluble factors produced by glia (Yang et al., 2003; Jones et al., 2011). Despite the differences, one common trend was observed across the different groups of cultures – the number of motifs was small compared to the amount of possible activation sites in the arrays – suggesting that the loci of burst initiation in uniform cultures were rather localized.

It was proposed that the spontaneous formation of repeating spatiotemporal motifs reflects the inherent neural mechanisms associated with learning and memory (Madhavan et al., 2007; Villette et al., 2015). The higher precision of conservation observed in the spatiotemporal motifs in HGC and LGC may therefore point to the importance of neuron-glia interactions in enhancing memory formation in the networks. The current experimental setting with varying glial density could serve as a useful platform for studying memory encoding mechanism at a population level.

Previous work had demonstrated on the modulation of neuronal activity dynamics by glia, including their spiking and bursting characteristics (Newman and Zahs, 1998; Boehler et al., 2007), synaptic efficacy (Pfrieger and Barres, 1997; Oliet et al., 2001; Araque and Navarrete, 2010), and synchronicity of network activity (Feldt et al., 2010; Huang et al., 2015), most of which through comparison of the activity of cultures with and without glia. In the current study, the differences in the activity dynamics of HGC and GFC was examined throughout the network development, in terms of their spatiotemporal patterns of bursts and network synchrony. Beyond that, notable differences were also observed in some of the network parameters between HGC and LGC, highlighting the importance of glial density in regulating network activity.

5.2 Future Directions

Further work can be performed to better understand the role of glial cells in the regulation of spatiotemporal activity dynamics of neuronal networks. Several potential ones are listed below.

5.2.1 Calcium Buffering

Calcium ions were known to be active signaling molecules in the neuronal system, which are important not only for intercellular communications among neurons (Penn et al., 2016), but also glial cells (Hirase et al., 2004; Russell, 2011). To better understand how glia regulate the spatiotemporal activity

patterns of neuronal circuits, one can modulate the calcium activity of glial cells. This activity can be inhibited through injection of calcium chelators that buffer intracellular calcium ions. In contrast, calcium signals can also be induced using caged calcium reagent.

5.2.2 Optogenetic Glia Manipulation

The optogenetic technique has previously been used to manipulate neuronal activity. Recent studies suggested that this cutting-edge technology can also be applied to selectively activate/ inhibit glia in the brains of living animals (Cho et al., 2016), allowing investigation of the *in vivo* role of glial cells in the nervous system. The current work can be extended using animal models to study changes in the neuronal activity dynamics in response to manipulation of glial activity through optogenetic stimulation, and to verify the findings of the current work in the *in vivo* setting.

CHAPTER 6

CONCLUDING REMARKS

The role of glial cells in the generation of recurring motifs has been studied using dissociated cortical cultures growing on MEAs. It is shown that recurring activity pattern is a general property of self-organizing neural networks which could develop even in the absence of glial cells. Nevertheless, glial cells were critical for the generation of high-precision motifs, and the genesis of the latter at the earlier stage of development was very much dependent on the density of glia in the networks. Besides, the findings of the current study also showed that neuro-glia interactions and the density of glia in the networks have profound effects on the spatiotemporal patterns of bursts and network synchrony.

REFERENCES

Anderson, C.M. and Swanson, R.A., 2000. Astrocyte glutamate transport: Review of properties, regulation, and physiological functions. *Glia*, 32(1), pp.1–14.

Araque, A. and Navarrete, M., 2010. Glial cells in neuronal network function. *Philosophical Transactions of the Royal Society B: Biological Sciences*, 365, pp.2375–2381.

Badura, A. et al., 2014. Fast calcium sensor proteins for monitoring neural activity. *Neurophotonics*, 1(2), pp.1–12.

Baruchi, I. and Ben-Jacob, E., 2007. Towards neuro-memory-chip: Imprinting multiple memories in cultured neural networks. *Physical Review E*, 75(5), pp.1–4.

Bikbaev, A., Frischknecht, R. and Heine, M., 2015. Brain extracellular matrix retains connectivity in neuronal networks. *Scientific Reports*, 5, pp.1–12.

Boehler, M.D., Wheeler, B.C. and Brewer, G.J., 2007. Added astroglia promote greater synapse density and higher activity in neuronal networks. *Neuron Glia Biology*, 5, pp.127–140.

Chever, O. et al., 2016. Astroglial networks promote neuronal coordination. *Science Signaling*, 9(410), pp.1–8.

Cho, W.-H., Barcelon, E. and Lee, S.J., 2016. Optogenetic glia manipulation: Possibilities and future prospects. *Experimental Neurobiology*, 25(5), pp.197–204.

Delcomyn, F., 1976. An approach to the study of neural activity during behaviour in insects. *Journal of Insect Physiology*, 22, pp.1223–1227.

Dichter, M.A., 1978. Rat cortical neurons in cell culture: culture methods, cell morphology, electrophysiology, and synapse formation. *Brain Research*, 149, pp.279–293.

Eroglu, C. and Barres, B.A., 2010. Regulation of synaptic connectivity by glia. *Nature*, 468, pp.223–231.

Feldt, S. et al., 2010. Functional clustering in hippocampal cultures: relating network structure and dynamics. *Physical Biology*, 7(4), pp.1–12.

Fujita, N. et al., 2013. Visualization of neural activity in insect brains using a conserved immediate early gene, Hr38. *Current Biology*, 23(20), pp.2063–2070.

Grienberger, C., Chen, X. and Konnerth, A., 2014. NMDA receptor-dependent multidendrite Ca^{2+} spikes required for hippocampal burst firing in vivo. *Neuron*, 81(6), pp.1274–1281.

Grienberger, C. and Konnerth, A., 2012. Imaging calcium in neurons. *Neuron*, 73(5), pp.862–885.

Hirase, H. et al., 2004. Two-photon imaging of brain pericytes in vivo using dextran-conjugated dyes. *Glia*, 46(1), pp.95–100.

Huang, Y.T., Chang, C.H., Lai, P.Y. and Chan, C.K., 2015. Effects of glia on the synchronized bursting in cultured neuronal networks. *Chinese Journal of Physics*, 53(4), pp.1–14.

Ikegaya, Y. et al., 2004. Synfire chains and cortical songs: Temporal modules of cortical activity. *Science*, 304, pp.559–564.

Izhikevich, E.M., Desai, N.S., Walcott, E.C. and Hoppensteadt, F.C., 2003. Bursts as a unit of neural information: Selective communication via resonance. *Trends in Neurosciences*, 26(3), pp.161–167.

Jimbo, Y. and Robinson, H.P.C., 2000. Propagation of spontaneous synchronized activity in cortical slice cultures recorded by planar electrode arrays. *Bioelectrochemistry and Bioenergetics*, 51(2), pp.107–115.

Jones, E. V. et al., 2011. Astrocytes control glutamate receptor levels at developing synapses through SPARC- -integrin interactions. *Journal of Neuroscience*, 31(11), pp.4154–4165.

Ju, H. et al., 2015. Spatiotemporal memory is an intrinsic property of networks of dissociated cortical neurons. *Journal of Neuroscience*, 35(9), pp.4040–4051.

Kaminsky, N., Bihari, O., Kanner, S. and Barzilai, A., 2016. Connecting malfunctioning glial cells and brain degenerative disorders. *Genomics, Proteomics and Bioinformatics*, 14(3), pp.155–165.

Kamioka, H. et al., 1996. Spontaneous periodic synchronized bursting during formation of mature patterns of connections in cortical cultures. *Neuroscience Letters*, 206(2–3), pp.109–112.

Knutson, B., Westdorp, A., Kaiser, E. and Hommer, D., 2000. FMRI visualization of brain activity during a monetary incentive delay task. *NeuroImage*, 12(1), pp.20–27.

Lampl, I., Reichova, I. and Ferster, D., 1999. Synchronous membrane potential fluctuations in neurons of the cat visual cortex. *Neuron*, 22, pp.361–374.

Latham, P.E., Richmond, B.J., Nirenberg, S.H. and Nelson, P.G., 2000. Intrinsic dynamics in neuronal networks. II. experiment. *Journal of Neurophysiology*, 83, pp.828–835.

Lee, A.K. and Wilson, M.A., 2002. Memory of sequential experience in the hippocampus during slow wave sleep. *Neuron*, 36(6), pp.1183–1194.

Lock, J.T., Parker, I. and Smith, I.F., 2016. A comparison of fluorescent Ca^{2+} indicators for imaging local Ca^{2+} signals in cultured cells. *Cell Calcium*, 58(6), pp.638–648.

Luczak, A. et al., 2007. Sequential structure of neocortical spontaneous activity in vivo. *Proceedings of the National Academy of Sciences*, 104(1), pp.347–352.

Madhavan, R., Chao, Z.C. and Potter, S.M., 2007. Plasticity of recurring spatiotemporal activity patterns in cortical networks. *Physical Biology*, 4(3), pp.181–93.

Madhavan, R., Chao, Z.C. and Potter, S.M., 2005. Spontaneous bursts are better indicators of tetanus-induced plasticity than responses to probe stimuli. *2nd International IEEE EMBS Conference on Neural Engineering*, 2005, pp.434–437.

Matsumoto, K., Ishikawa, T., Matsuki, N. and Ikegaya, Y., 2013. Multineuronal spike sequences repeat with millisecond precision. *Frontiers in Neural Circuits*, 7(112), pp.1–12.

Mok, S.Y., Nadasdy, Z., Lim, Y.M. and Goh, S.Y., 2012. Ultra-slow oscillations in cortical networks in vitro. *Neuroscience*, 206, pp.17–24.

Mokeichev, A. et al., 2007. Stochastic emergence of repeating cortical motifs in spontaneous membrane potential fluctuations in vivo. *Neuron*, 53(3), pp.413–425.

Nádasdy, Z. et al., 1999. Replay and Time Compression of Recurring Spike Sequences in the Hippocampus. *The Journal of Neuroscience*, 19(21), pp.9497–9507.

Newman, E.A., 2015. Glial cell regulation of neuronal activity and blood flow in the retina by release of gliotransmitters. *Philosophical Transactions of the Royal Society B*, 370, pp.1–9.

Newman, E.A. and Zahs, K.R., 1998. Modulation of neuronal activity by glial cells in retina. *Journal of Neuroscience*, 18(11), pp.4022–4028.

Oliet, S.H.R., Piet, R. and Poulain, D.A., 2001. Control of glutamate clearance and synaptic efficacy by glial coverage of neurons. *Science*, 292, pp.923–926.

Oyelade, O.J., Oladipupo, O.O. and Obagbuwa, I.C., 2010. Application of k Means Clustering algorithm for prediction of Students Academic Performance. *International Journal of Computer Science and Information Security*, 7(1), pp.292–295.

Pasquale, V. et al., 2008. Self-organization and neuronal avalanches in networks of dissociated cortical neurons. *Neuroscience*, 153(4), pp.1354–1369.

Pasquale, V., Martinoia, S. and Chiappalone, M., 2017. Stimulation triggers endogenous activity patterns in cultured cortical networks. *Scientific Reports*, 7(9080), pp.1–16.

Penn, Y., Segal, M. and Moses, E., 2016. Network synchronization in hippocampal neurons. *Proceedings of the National Academy of Sciences*, 113(12), pp.3341–3346.

Perea, G. and Araque, A., 2010. GLIA modulates synaptic transmission. *Brain Research Reviews*, 63(1–2), pp.93–102.

Pfrieger, F.W. and Barres, B.A., 1997. Synaptic efficacy enhanced by glial cells in vitro. *Science*, 277, pp.1684–1687.

Phatnani, H. and Maniatis, T., 2015. Astrocytes in neurodegenerative disease. *Cold Spring Harbor Perspectives in Biology*, 7(6), pp.1–17.

Potter, S.M., 2001. Distributed processing in cultured neuronal networks. *Progress in Brain Research*, 130, pp.49–62.

Powell, E.M. and Geller, H.M., 1999. Dissection of astrocyte-mediated cues in neuronal guidance and process extension. *Glia*, 26(1), pp.73–83.

Raichman, N. and Ben-Jacob, E., 2008. Identifying repeating motifs in the activation of synchronized bursts in cultured neuronal networks. *Journal of Neuroscience Methods*, 170(1), pp.96–110.

Reppel, M. et al., 2004. Microelectrode arrays: A new tool to measure embryonic heart activity. *Journal of Electrocardiology*, 37, pp.104–109.

Rey, H.G., Pedreira, C. and Quian Quiroga, R., 2015. Past, present and future of spike sorting techniques. *Brain Research Bulletin*, 119, pp.106–117.

Rolston, J.D., Wagenaar, D.A. and Potter, S.M., 2007. Precisely timed spatiotemporal patterns of neural activity in dissociated cortical cultures. *Neuroscience*, 148(1), pp.294–303.

Russell, J.T., 2011. Imaging calcium signals in vivo: A powerful tool in physiology and pharmacology. *British Journal of Pharmacology*, 163(8), pp.1605–1625.

Sasaki, T. et al., 2014. Astrocyte calcium signalling orchestrates neuronal synchronization in organotypic hippocampal slices. *The Journal of Physiology*, 592(13), pp.2771–2783.

Schroeter, M.S. et al., 2015. Emergence of rich-club topology and coordinated dynamics in development of hippocampal functional networks in vitro. *Journal of Neuroscience*, 35(14), pp.5459–5470.

Schwartzkroin, P.A., Baraban, S.C. and Hochman, D.W., 1998. Osmolarity, ionic flux, and changes in brain excitability. *Epilepsy Research*, 32(1–2), pp.275–285.

Segev, R., Baruchi, I., Hulata, E. and Ben-Jacob, E., 2004. Hidden neuronal correlations in cultured networks. *Physical Review Letters*, 92(11), pp.1–4.

Sibarov, D.A., Abushik, P.A., Giniatullin, R. and Antonov, S.M., 2016. GluN2A subunit-containing NMDA receptors are the preferential neuronal targets of homocysteine. *Frontiers in Cellular Neuroscience*, 10, pp.1–11.

Srivastava, K.H. et al., 2017. Motor control by precisely timed spike patterns. *Proceedings of the National Academy of Sciences*, 114(5), pp.1171–1176.

Stark, E., Asher, I. and Abeles, M., 2007. Encoding of Reach and Grasp by Single Neurons in Premotor Cortex Is Independent of Recording Site. *Journal of Neurophysiology*, 97(5), pp.3351–3364.

Stogsdill, J.A. and Eroglu, C., 2017. The interplay between neurons and glia in synapse development and plasticity. *Current Opinion in Neurobiology*, 42, pp.1–8.

Sun, J.-J., Kilb, W. and Luhmann, H.J., 2010. Self-organization of repetitive spike patterns in developing neuronal networks in vitro. *European Journal of Neuroscience*, 32(8), pp.1289–1299.

Supèr, H. and Roelfsema, P.R., 2004. Chronic multiunit recordings in behaving animals: Advantages and limitations. *Progress in Brain Research*, 147(SPEC. ISS.), pp.263–282.

Takayama, Y., Moriguchi, H., Kotani, K. and Jimbo, Y., 2009. Spontaneous calcium transients in cultured cortical networks during development. *IEEE Transactions on Biomedical Engineering*, 56(12), pp.2949–2956.

Tropp Sneider, J. et al., 2006. Differential behavioral state-dependence in the burst properties of CA3 and CA1 neurons. *Neuroscience*, 141(4), pp.1665–1677.

Tsacopoulos, M. and Magistretti, P.J., 1996. Metabolic coupling between glia and neurons. *The Journal of Neuroscience*, 16(3), pp.877–85.

Villette, V. et al., 2015. Internally recurring hippocampal sequences as a population template of spatiotemporal information. *Neuron*, 88(2), pp.357–366.

Wagenaar, D.A., Demarse, T.B. and Potter, S.M., 2005. MEABench : A toolset for multi-electrode data acquisition and on-line analysis MeaBench. *Proceedings of the 2nd International IEEE EMBS Conference of Neural Engineering*, pp.5–8.

Wagenaar, D.A., Madhavan, R., Pine, J. and Potter, S.M., 2005. Controlling bursting in cortical cultures with closed-loop multi-electrode stimulation. *Journal of Neuroscience*, 25(3), pp.680–688.

Wagenaar, D.A., Pine, J. and Potter, S.M., 2006. An extremely rich repertoire of bursting patterns during the development of cortical cultures. *BMC Neuroscience*, 7(1), pp.1–18.

Yada, Y., Kanzaki, R. and Takahashi, H., 2016. State-dependent propagation of neuronal sub-population in spontaneous synchronized bursts. *Frontiers in Systems Neuroscience*, 10(28), pp.1–13.

Yamashita, E.Y., 2005. Using a K-Means Clustering Algorithm to examine patterns of pedestrian involved crashes in Honolulu , Hawaii. *Journal of Advanced Transportation*, 41(1), pp.69–89.

Yang, Y. et al., 2003. Contribution of astrocytes to hippocampal long-term potentiation through release of D-serine. *Proceedings of the National Academy of Sciences of the United States of America*, 100(25), pp.15194–15199.

Zhang, J.M. et al., 2003. ATP released by astrocytes mediates glutamatergic activity-dependent heterosynaptic suppression. *Neuron*, 40(5), pp.971–982.

Zotev, V. et al., 2014. Self-regulation of human brain activity using simultaneous real-time fMRI and EEG neurofeedback. *NeuroImage*, 85, pp.985–995.

APPENDIX A

CELL CULTURING AND IMMUNOSTAINING PROTOCOLS

This section provides the details of the cell culturing and immunostaining protocols used in this study.

Cell Dissociation

Dissected cortical tissues from E18 Sprangue Dawley Rat (BrainBits^{TM}) were transferred into recently thawed 0.25% trypsin. After enzymatic digestion for 15 minutes at 37˚C, they were transferred into Hank's balanced salt solution with 10% Equine serum and mechanically triturated by 10-15 passes through a 1 mL pipette tip, in sets of 3. Between each set, the clumps were let settled down and the suspended cells were transferred to a new sterile tube. Then, the dissociated cells were centrifuged onto bovine serum albumin (1% in 1X PBS) at 150 x g for 6 minutes and the resulting pellet was resuspended in serum-supplemented medium. Cells were diluted with serum-supplemented medium to achieve a final concentration of 4000 cells/µL. For the cultures of reduced neuronal density, the cells were diluted to a final concentration of 2400 cells/µL.

Preparation of MEA Surface

The MEAs were first cleaned with 2% Tergazyme solution for 30 minutes and rinsed thoroughly with double-distilled water (ddH_2O). After rinsing, the MEAs were autoclaved at 121 ˚C for 20 minutes. The MEAs were then left to air-dry inside the biosafety cabinet. Following this, they were added with 750 mL of PEI solution each and kept at 37 ˚C incubator for overnight incubation. On the subsequent day, after the PEI was withdrawn, the MEAs were washed with sterile ddH_2O for at least 3 times, with 1-2 mL each time. They were left inside the biosafety cabinet until they were completely dry. All the MEAs were exposed to UV for 15 minutes before use.

Preparation of PEI Solution

To prepare PEI solution, 0.05% PEI (volume/volume) was mixed with borate buffer solution (3.1 g boric acid and 4.75 g borax in 1 L ddH_2O, pH 8.4). The PEI solution was filtered-sterilized at 0.2 μm before adding to MEAs.

Cell Plating

The cell suspension was mixed thoroughly with a vortex mixer for 10 seconds. Then, the cells were seeded in a 50 μL drop on central area of MEAs precoated with PEI. All MEAs were covered with Teflon membrane and incubated at 37˚C, 5% CO_2 for 2 hours to allow the cells to attach to the substratel. After 2 hours, 1 mL of serum-supplemented medium was added to

each MEA.

Cell Maintenance

On DIV 7, half of the medium in HGC and LGC was replaced with the same amount of serum-supplemented medium, whereas half of the medium in GFC was replaced with the same amount of glial-conditioned medium. In the subsequent medium replacement, similar changes were carried out on every 4 to 7 days to all culture groups, depending on the color changes of the medium.

Preparation of Serum-supplemented and Serum-free Medium

The following table described the recipe for serum-supplemented and serum-free medium.

Reagents	Quantity (mL)	
	Serum-supplemented medium	Serum-free medium
Neurbasal medium	45	47.5
Equine serum	2.5	-
Glutamax	0.13	0.13
B27	1	1

Preparation of Glial-conditioned Medium

Glial-conditioned medium contained glial-secreted factors that can partly mimic the effect of glial cells and has been shown to be important in maintaining the and neuronal health of GFC (Boehler et al., 2007). To obtain

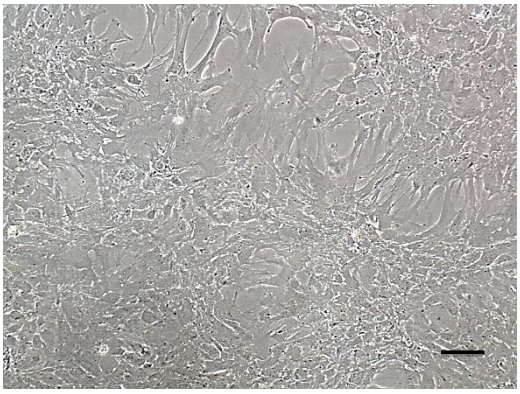

Figure A: Phase contrast micrograph of a purified glial culture at fourth weeks *in vitro*. Scale bar: 100 µm.

glial-conditioned medium, cortical tissues of E18 embryonic rats were dissociated using the same protocol described above. The dissociated cells were resuspended in Neurobasal medium supplemented with 5% Equine serum and 1 mM Glutamax. The cell suspension was then diluted to 7500 cells/ mL and plated on 25 cm^2 culture flasks. Once the glial cells formed a confluent layer (Figure A), a full serum-free medium change was performed and the medium was collected after 24 hours.

Immunostaining

The final concentration of cells used for immunostaining experiments was 300 cells/µL. Cells (in 200 µL suspension) were added and spread evenly on the central area of glass bottom dishes that had been pretreated with PEI, and maintained in their respective medium. On the days of experiment, the cultures were washed with 1X PBS twice to wash away the floating residuals. The cultures were then fixed with 250 µL of 4% paraformaldehyde for 10 minutes. After washing the paraformaldehyde with 1X PBS three times, the cultures were permeabilized with 250 µL of 0.03% Triton X-100 for 5

minutes. The cultures were then washed with 1X PBS thrice and treated with 500 µL of 5% bovine serum albumin for 30 minutes to reduce the background.

Subsequently, the bovine serum albumin was removed, and the cultures were incubated with 200 µL of primary antibodies (mixture of anti-MAP2 (chicken, 1:1000) and anti-GFAP (mouse, 1:1000) in 1X PBS) at room temperature for 1 hour. The cultures were then washed with 1X PBS three times for 5 minutes each. This is to ensure that the excessive primary antibodies were removed to reduce background fluorescence. The cultures were exposed to 200 µL of secondary antibodies (mixture of Alexa Fluor 488 goat-anti-chicken (1:200) and Alexa Fluor 546 goat-anti-mouse (1:200) in 1X PBS) at room temperature for 45 minutes. The incubation was performed in the dark. The cultures were then washed with 1X PBS three times for 5 minutes each to remove any excessive secondary antibodies. They were counterstained with 200 µL of 1 µg/mL DAPI for 1 minute and washed with 1X PBS thrice. Lastly, the cultures were mounted with few drops of Fluoromount and allowed to dry. Images were captured using a Nikon fluorescence microscope.

Details of Chemicals

The names of the chemicals, their respective brands and catalog numbers are described in the table below.

Chemicals name	Brands	Catalog no.
0.25% Trypsin	Life Technologies	25200058
Alexa Fluor 488 goat-anti-chicken	Life Technologies	A11039
Alexa Fluor 546 goat-anti-mouse	Life Technologies	A11030
Anti-GFAP	Merck Millipore	MAB3402
Anti-MAP2	Abcam	AB5392
Ara-C	Sigma	C1768
B27	Life Technologies	17604044
Boric acid	Fisher Scientific	A73500
Bovine serum albumin	Sigma	A4503
DAPI	Sigma	D9542
Equine serum	HyClone Laboratories	SH30074
Fluoromount	Sigma	F4580
Glutamax	Life Technologies	35050061
Hank's balanced salt solution	Life Technologies	14170112
Neurobasal medium	Life Technologies	21103049
Paraformaldehyde	Sigma	P6148
Phosphate buffered saline	Life Technologies	70011044
Poly-ethylene-imine	Sigma	P3143
Borax (sodium tetraborate)	Sigma	B0127
Triton X-100	Sigma	T8787